JGR Biogeosciences

RESEARCH ARTICLE
10.1029/2023JG007831

Composition and Bioreactivity of Dissolved Organic Matter Leachates From End Members in a Mountain to Prairie Transitional River Valley

Xingzi Zhou[1], Laura A. Logozzo[1], Sarah Ellen Johnston[1,2], Lauren Zink[1], Armi-Lee Amerila[1], and Matthew J. Bogard[1]

[1]Department of Biological Sciences, University of Lethbridge, Lethbridge, AB, Canada, [2]Now at Department of Chemistry and Biochemistry, University of Alaska Fairbanks, Fairbanks, AK, USA

Key Points:

- Bioavailability of end member leachates increased from soils to river sources (fish, then macrophytes and biofilm), to terrestrial plants
- Dissolved organic matter (DOM) composition and bioavailability were modestly responsive to elevated discharge during the spring freshet
- Weakly bioavailable soil DOM dominated the downstream river pool, possibly showing the mainstem is not a hotspot for DOM transformation

Supporting Information:

Supporting Information may be found in the online version of this article.

Correspondence to:

M. J. Bogard,
matthew.bogard@uleth.ca

Citation:

Zhou, X., Logozzo, L. A., Johnston, S. E., Zink, L., Amerila, A.-L., & Bogard, M. J. (2024). Composition and bioreactivity of dissolved organic matter leachates from end members in a mountain to prairie transitional river valley. *Journal of Geophysical Research: Biogeosciences*, *129*, e2023JG007831. https://doi.org/10.1029/2023JG007831

Received 2 OCT 2023
Accepted 28 MAY 2024

Author Contributions:

Conceptualization: Xingzi Zhou, Sarah Ellen Johnston, Matthew J. Bogard
Data curation: Xingzi Zhou, Laura A. Logozzo, Lauren Zink, Matthew J. Bogard
Formal analysis: Xingzi Zhou, Laura A. Logozzo
Funding acquisition: Sarah Ellen Johnston, Matthew J. Bogard
Investigation: Xingzi Zhou, Laura A. Logozzo, Sarah Ellen Johnston, Lauren Zink, Armi-Lee Amerila, Matthew J. Bogard
Methodology: Xingzi Zhou, Laura A. Logozzo, Sarah Ellen Johnston,

Abstract River organic matter transformations impact the cycling of energy, carbon, and nutrients. The delivery of distinct dissolved organic matter (DOM) sources can alter aquatic DOM cycling and associated biogeochemical processes. Yet DOM source and reactivity are not well-defined for many river systems, including in western Canada. Here, we explore DOM cycling in the mainstem of the Oldman River (stream order 6–7), a heavily regulated river network in southern Alberta (Canada). We compared seasonal river DOM content, composition, and bioavailability with nine endmember leachates from the river valley using optical properties and incubations to estimate biodegradable dissolved organic carbon (BDOC). River DOM composition was most similar to terrestrial soil leachates, followed by autochthonous DOM leachates. River DOM bioavailability was low (BDOC = 0%–16.6%, mean of 7.1%). Endmember leachate bioavailability increased from soils (BDOC = 23.9%–53.7%), to autochthonous sources (fish excretion, macrophytes, biofilm; BDOC = 49.9%–80.0%), to terrestrial vegetation (leaves, shrubs, grass; BDOC > 80%), scaling positively with protein-like DOM content and amount of leachable dissolved organic carbon (DOC), and negatively with aromaticity. Seasonally, DOC concentrations changed little despite >15-fold increases in discharge during spring. River DOM composition shifted modestly toward soil-like endmembers in spring and more bioavailable autochthonous end members in autumn and winter. Low DOM bioavailability in the river mainstem and low DOC yields shown in previous work point to limited internal processing of DOM and limited bioavailable DOM delivery to downstream habitats, possibly due to upstream flow regulation. Our observations provide important insights into the functioning of western Canadian aquatic networks.

Plain Language Summary Rivers are among the most heavily disturbed ecosystems worldwide. In agricultural regions of western Canada, human impacts on river ecosystem structure and functioning are not well defined. The study of organic matter chemistry provides important insights into aquatic ecosystem properties and biogeochemical processes. Here, we explore the seasonal trends in composition and content of dissolved organic matter in one of Canada's most heavily regulated rivers (the Oldman River, Alberta). While land use impacts on river organic matter cycling are documented elsewhere, we provide unique insights by tracking changes in river organic matter composition and microbial consumption across a complete annual cycle that includes winter. The composition and content of river organic matter changed little among seasons. Compared to potential organic matter sources from the river valley (soils, plants, aquatic organisms, and biofilm), river water had organic matter that mostly resembled soil sources, and secondarily river sources. Compared to all potential sources, river organic matter was less bioavailable to microbes and on the low end of bioavailability relative to other global aquatic systems. We hypothesize that human alterations to the flow regime upstream (including damming and irrigation) may dampen seasonal changes in river organic matter composition and cycling.

1. Introduction

Rivers are dynamic ecosystems that support complex food webs (Battin et al., 2016; Thorp et al., 2006; Vannote et al., 1980). Most of the world's rivers are impacted by human land use and hydrologic regulation (Grill et al., 2019; Vorosmarty et al., 2010). These impacts can modify the cycling of riverine dissolved organic matter (DOM) through multiple mechanisms that alter the rates and sources of external inputs, the chemical composition of DOM, and rates of internal DOM cycling (Butman et al., 2016; Maavara et al., 2020; Stanley et al., 2012; Xenopoulos et al., 2021). The cycling of DOM in aquatic ecosystems plays a central role in energy flows,

Lauren Zink, Armi-Lee Amerila, Matthew J. Bogard
Project administration: Xingzi Zhou, Matthew J. Bogard
Resources: Xingzi Zhou, Matthew J. Bogard
Software: Xingzi Zhou, Laura A. Logozzo
Supervision: Laura A. Logozzo, Sarah Ellen Johnston, Matthew J. Bogard
Validation: Xingzi Zhou, Laura A. Logozzo, Matthew J. Bogard
Visualization: Xingzi Zhou, Laura A. Logozzo
Writing – original draft: Xingzi Zhou, Matthew J. Bogard
Writing – review & editing: Xingzi Zhou, Laura A. Logozzo, Sarah Ellen Johnston, Lauren Zink, Matthew J. Bogard

biogeochemical processes including nutrient and carbon (C) cycling, and other important ecosystem features (Carlson & Hansell, 2015; Fellman et al., 2010; Findlay & Sinsabaugh, 2003). The dynamic flow regimes of rivers make it difficult to define the human impacts on DOM loading and processing (e.g., Vaughn et al., 2021; Wagner et al., 2015). We know even less about the annual phenology of river DOM processing, and many global regions remain understudied with respect to aquatic DOM biogeochemistry, including the rivers of western Canada (the focus of this study).

The transformations of DOM through a river network depend, in part, on DOM composition and bioavailability, which vary widely through space (i.e., along individual stream reaches and across watersheds) and time (Begum et al., 2023; Butman et al., 2012; Hutchins et al., 2017; Wilson & Xenopoulos, 2008). Allochthonous, externally derived DOM (the bulk of the riverine OM pool (Findlay & Sinsabaugh, 2003; Tank et al., 2018)) is generally more aromatic and less bioavailable compared to autochthonous, in situ DOM (del Giorgio & Davis, 2003; del Giorgio & Pace, 2008). Therefore, external DOM inputs shape the composition and transformation rates of the riverine DOM pool (A. A. Coble et al., 2016; Tank et al., 2018). The composition and bioavailability of allochthonous DOM in rivers can be affected by land use and landscape features including, but not limited to: (a) wetland cover in a watershed and wetland conditions (Camino-Serrano et al., 2014; Xenopoulos et al., 2003), (b) photo- and biodegradation of vegetation and soil organic carbon stocks (Camino-Serrano et al., 2014; Singh et al., 2014; Thieme et al., 2019), and (c) types of soil (e.g., organic- vs. mineral rich soils) and soil conditions (moisture, temperature, and stoichiometry) (Aitkenhead & McDowell, 2000; Kaiser & Kalbitz, 2012; Kindler et al., 2011; Tank et al., 2018; van den Berg et al., 2012). In general, watershed wetland cover and the presence of organic rich soils and shallow terrestrial flow paths increase aromatic DOM export to rivers, while photo-degradation of leaf litter, the dominance of mineral soils, and engagement of deeper flow paths can decrease aromatic DOM export to rivers (Camino-Serrano et al., 2014; Kaiser & Kalbitz, 2012; Tank et al., 2018). Terrestrial vegetation provides additional dissolved organic carbon (DOC) and labile DOM to soils and rivers, but this input varies by stream order (e.g., Chauvet, 1997; Vannote et al., 1980), as well as vegetation type and previous exposure to microbial processes (Camino-Serrano et al., 2014; Lidman et al., 2017; Thieme et al., 2019). Hydrological events such as storms increase the lateral export of aromatic allochthonous DOM to rivers through increased shallow and sub-surface soil flows (Raymond et al., 2016; Shultz et al., 2018), whereas autochthonous DOM dominates in large rivers, at low flows, and in drought (Hosen et al., 2019, 2020). Given the numerous factors controlling the quantity and quality of allochthonous DOM in rivers, the patterns of terrestrial DOM cycling vary spatially and temporally in ways that are not fully understood.

Compared to allochthonous DOM, autochthonous DOM is generally less aromatic, more aliphatic, with lower molecular weight and greater bioavailability compared to soil-derived DOM (Asmala et al., 2013; del Giorgio & Pace, 2008; Findlay & Sinsabaugh, 2003). Autochthonous DOM is largely derived from biofilm, phytoplankton, macrophytes, and aquatic animals (Lapierre & Frenette, 2009; Romaní et al., 2004; Sabater et al., 2007). Biofilms (complex benthic attached communities including phytoplankton, bacteria, protozoa, fungi, and benthos; (Battin et al., 2016)) can uptake large quantities of C and nutrients (Costerton, 1999; Flemming, 1995; Kamjunke et al., 2015; Sabater et al., 2007). The DOM released from biofilms can vary in composition (Flemming, 1995; Romaní et al., 2004), and protozoan grazing leads to rapid turnover of biofilm organic matter (Risse-Buhl et al., 2012). Both phytoplankton and macrophytes release DOM that is highly bioavailable, as it is rich in aliphatic compounds and protein-like DOM (Hansen et al., 2016; Mangal et al., 2016; Zhang et al., 2013). Recent studies have reported that DOM excreted by aquatic animals such as fish (Q. Liu et al., 2022) and zooplankton (Johnston, Finlay, et al., 2022; Maas et al., 2020), and DOM leached from their faeces, can supply bioavailable organic nutrients (C, N, phosphorus (P)) to aquatic ecosystems (Parr et al., 2018; Schmitz et al., 2014). Ultra-high resolution characterization of zooplankton DOM leachate showed hundreds of biolabile molecular formulas that were undetected in ambient lake water and likely rapidly consumed by microbes upon excretion (Johnston, Finlay, et al., 2022). Although most bioavailable, autochthonous DOM is consumed and does not persist long in aquatic ecosystems, the excretion and recycling of DOM from distinct autochthonous sources (e.g., biofilm, zooplankton, fish) may have unique chemical features that potentially affect the composition and bioavailability of DOM cycling at the ecosystem level. However, the impact of internally derived DOM on riverine processes can be difficult to discern based on bulk dissolved organic carbon (DOC) measurements, given that riverine microbial communities can preferentially consume autochthonous DOM while exporting comparatively large quantities of allochthonous DOM downstream (del Giorgio and Pace, 2008).

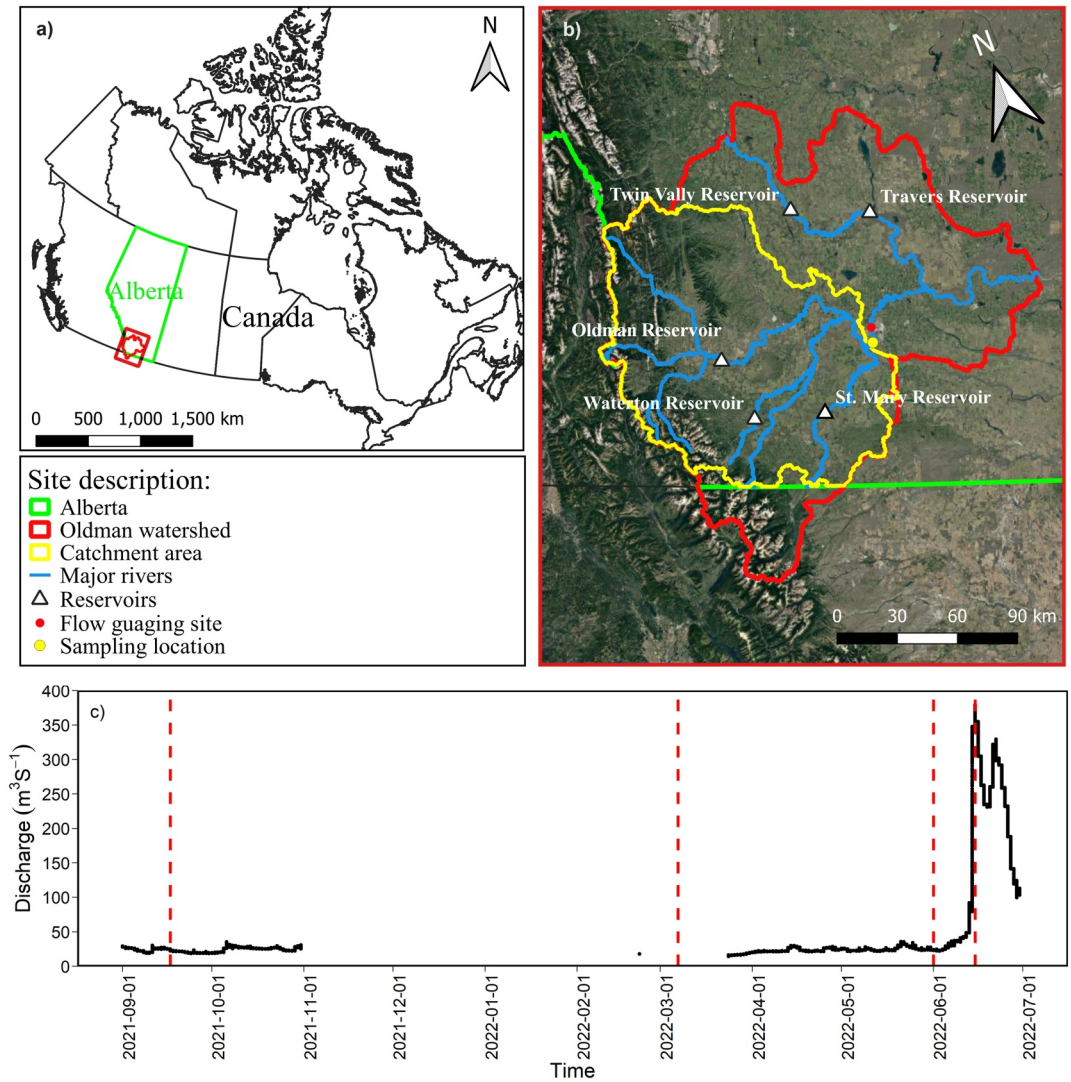

Figure 1. Location of sampling site in the Oldman Watershed (OMW), Alberta, Canada and discharge at the Oldman River near Lethbridge. (a) Location of the OMW in Canada, (b) the major rivers and the sampling site in the OMW, and (c) Discharge at the Oldman River near Lethbridge (05AD007) from 01 September 2021 to 01 July 2022, with the sampling dates shown as red dashed lines. Discharge is not monitored in winter months due to ice cover on the river. Google satellite reference: EPSG:3857—WGS 84/Pseudo-Mercator—Projected.

Semi-arid and arid regions make up nearly a third of all land area (Wickens, 1998); rivers in these regions are often heavily regulated due to limited water supply, such that nearly all semi-arid rivers are impounded. Impoundments increase network-scale residence time and potentially DOM uptake (Du et al., 2021). For example, at the network scale, DOM biomineralization in a temperate watershed predominantly occurred in connected lakes and reservoirs (~80%, Maavara et al., 2023), thereby controlling downstream DOM export and composition (Miller, 2012; Ulseth & Hall, 2015). While many studies have documented the composition of individual sources of riverine DOM and the potential roles that both terrestrial and aquatic sources of DOM can play in river energetics and biogeochemistry, little is known about these features in highly regulated, semi-arid rivers, especially in Canada. In fact, a recent global analysis of river DOM biodegradation rates did not include any semi-arid rivers (F. Liu & Wang, 2022), demonstrating the need for estimates to fill this knowledge gap.

Here, we explore riverine DOM cycling in one of Canada's most heavily regulated ecosystems (the Oldman River in the South Saskatchewan River Basin; Figure 1a). Throughout the southern portion of the three western Prairie provinces of Canada, Rocky Mountain headwaters deliver the bulk of DOM to downstream river reaches in the northern Great Plains (Johnston, Gunawardana, et al., 2022). Intense downstream land and water use, and heavy

flow regulation severely impact the hydrology and biogeochemistry of western Canadian rivers (Schindler, 2001, 2019; Tan & Gan, 2015). In other large river systems, upstream impoundment and flow regulation have been shown to enhance autochthonous contributions and in situ DOM processing, thereby stabilizing the temporal changes in composition and processing of DOM in downstream river reaches (Oliver et al., 2016; Ulseth & Hall, 2015). We hypothesized that a similar pattern of seasonal stabilization of DOM content and composition may exist in the heavily regulated Oldman River. To detail DOM cycling in the mainstem of the Oldman River Basin, we selected a mainstem reach of the Oldman River downstream of the Oldman reservoir as a case study to define: (a) the chemical composition and potential microbial reactivity of distinct river valley DOM sources, (b) seasonal dynamics of riverine DOM composition and microbial consumption of DOM, and (c) the relative contributions from distinct DOM endmember sources to river DOM.

2. Methods

2.1. Oldman Watershed and Sampling Site Description

The Oldman Watershed (OMW) (Figure 1b) has a catchment area of 28,000 km^2 that is made up of ~33% agricultural land use, 29% forest cover, and 17% native vegetation cover (Johnston, Gunawardana, et al., 2022; Tanzeeba & Gan, 2012). The watershed is home to more than 160,000 people with the majority living in the city of Lethbridge, Alberta, Canada (Byrne et al., 2006; Koning et al., 2006). The Oldman River network flows from its headwaters in the Rocky Mountains in south-western Alberta, Canada and northern Montana, USA toward the east, joining the Bow River to form the South Saskatchewan River at Medicine Hat, with water eventually flowing into Hudson Bay (Figure 1b) (Byrne et al., 2006; Koning et al., 2006). The watershed is situated in a semi-arid climatic region with low humidity. The mean river water temperature is between 3°C and 6°C and mean annual precipitation in the region ranges from 380 to 580 mm yr^{-1} (Rock & Mayer, 2007).

Intensification of land and water use over the past century in the OMW has led to substantial changes in watershed hydrology, similar to impacts throughout the wider western Canadian Prairie region (Schindler, 2001; Tan & Gan, 2015). Streamflow in the Oldman River decreased by ~34% from 1913 to 2003 (Rock & Mayer, 2007), and flow within the Castle Watershed, a mountainous headwater sub-basin, decreased by ~26% from 1949 to 2003 as a function of declining snow pack and glacial ice volume (Byrne et al., 2006). Flows in the watershed are heavily regulated, with ~87% of flows used for irrigation (Byrne et al., 2006; Koning et al., 2006; Rock & Mayer, 2006).

We used a fixed sampling location within the OMW in the City of Lethbridge (Popson Park; latitude: 49.641°N, longitude: 112.854°W; Figure 1b). At this location in the basin, the river is an order 6–7 stream (Jokinen et al., 2012), and the estimated upstream catchment area is 14,651 km^2, as determined from the Government of Alberta Flow Estimation Tool for Ungauged Watersheds (https://afetuw.alberta.ca/). The St. Mary and Belly Rivers originating in the Rocky Mountains contribute 38% of the total flow at our sampling site (Byrne et al., 2006; Cross & Anderson, 1989). The averaged total annual natural flow near Lethbridge is 2.19 km^3 yr^{-1}, with an annual DOC flux of 7.19 ± 4.47 Gg C yr^{-1} (Johnston, Gunawardana, et al., 2022), and with water temperature ranging annually from 0°C to 26°C (Alberta Environment, 2007; Cross & Anderson, 1989). Over the annual sampling cycle, the mean discharge rate was 47.3 ± 70.9 m^3 s^{-1} (from 1 September 2021 to 30 June 2022; Gauging Station ID: 05AD007, latitude: 49.709°N, longitude: 112.863°W; Figure 1c). The average flow on each sampling day was 23.2 ± 0.7 m^3 s^{-1} on 17 September 2021, unrecorded due to ice cover on 7 March 2022, 22.5 ± 0.2 m^3 s^{-1} on 1 June 2022, and 360.9 ± 12.1 m^3 s^{-1} on 15 June 2022. The mean daily discharge during the ice-free period (i.e., excluding 1 November 2021–23 March 2022) ranged from 15.8 to 360.9 m^3 s^{-1} throughout the complete river sampling cycle (1 September 2021–30 June 2022, Figure 1c).

2.2. River Water Sample Collection

We collected ambient river water samples for chemical analyses from the Oldman River at Popson Park (Figure 1b) on 17 September 2021 (autumn), 7 March 2022 (winter), 1 June 2022 (spring, low flow), and 15 June 2022 (spring, high flow during freshet). At the same time, we collected water for conducting biodegradable DOC (BDOC) incubations upon returning to the lab (details are listed below). All microorganisms were removed by filtering river water through 0.2 μm membrane filters (PALL Supor 200) into 4L acid washed Nalgene bottles to eliminate biodegradation during storage, and filtrates were stored in the dark at 4°C to further minimize any DOM transformation until initiation of incubations within 24 hr. For the 2 days leading up to the spring high flow sampling period, discharge increased from 70.9 to 360.9 m^3 s^{-1} (Figure 1c), because of intense spring

precipitation. Summed precipitation for the 48-hr period preceding the four sampling dates were 0, 0.4, 0.2, and 78.1 mm with average air temperatures of 10.73, −5.0, 11.4, and 10.3°C, respectively (City of Lethbridge meteorological station; climate ID 3033857; Alberta Agriculture and Forestry).

2.3. Leachate Sample Collection

We initiated the leachate BDOC experiments between 17 and 23 September 2021. To explore the differences in source DOM chemistry and potential bioavailability, we selected potential sources of DOM that likely contribute to the DOM pool of the Oldman River. This included both allochthonous (plants, soils) and autochthonous parent materials (biofilms, macrophytes, fish). All terrestrial parent materials were collected near the riverine sampling site. We collected three surface (top ∼5 cm) soil samples from upper, mid-, and riparian river valley soil layers, reflecting grassland, glacial till, and riparian cottonwood forest soils, respectively (Flanagan et al., 2017). Riparian soil samples (RS) were collected at the bottom of the river valley adjacent to the river, at the mid point (MS) of the valley halfway up the bank where an abundance of vegetation was located, and at the top of river valley (TS), where only grass was observed. We sieved soil samples through 500 μm mesh to remove large particles and dead vegetation. The vegetation samples included leaves from cottonwood trees (LE; Populus spp.), mixed riparian shrub materials (RV), which include *Medicago alfalfa*, and *Salix exigua*; and riparian grass (GR), *Carex* sedges. To collect biofilm (BF), we scrubbed rocks from the riverbed (Farag et al., 2007), brushed the biofilm into a pre-combusted wide mouth glass jar, and rinsed with ultrapure water during brushing (Farag et al., 2007). We collected macrophytes (MA) slightly downstream from Popson Park and gently rinsed with ultrapure water. All samples describe above (except the biofilm) were dried in an oven at 50°C until samples reached a constant weight (Johnston et al., 2019), while the biofilm was stored at 4°C before initiating the leaching process.

We collected fish excretion (FE) products from Fathead minnows (*Pimephales promelas*) that we caught using minnow traps within a storm-pond that is adjacent to the Oldman River, situated at the University of Lethbridge (latitude: 49.681°N, longitude: 112.870°W). Fathead minnows are an ideal fish species for determining the potential role of FE products on DOM diversity and bioavailability, as they are widely distributed throughout North America. Such wide distribution is due to their high tolerance for various environmental conditions and low selectivity of food (Ankley & Villeneuve, 2006; Duffy, 1998). They are well-studied in terms of their food preferences, gut microbial composition, and position and role within the food web (Ankley & Villeneuve, 2006; Duffy, 1998). All minnows were quickly rinsed using ultrapure water and transferred into a 4L acid-washed Nalgene bottles containing 500 ml 0.001M $NaHCO_3$ for a 10–15 min excretion incubation to collect FE. Following the incubation, we released the fathead minnows back to the pond, and the procedure was repeated three times to obtain enough excretion products for further analyses. The mixture solution after the excretion incubation was transferred into a pre-combusted wide mouth glass with 500 ml 0.001M $NaHCO_3$ to make up 1L 0.001M $NaHCO_3$ for the leaching process (Johnston et al., 2019).

Leachable DOM was then extracted from both allochthonous and autochthonous parent materials. About 5 g of LE, RV, GR, and MA, and 100 g of each soil sample (dry weight) and the BF solution was placed into wide mouth glass jars and stored in the dark at room temperature (21–23.5°C) for leaching (Johnston et al., 2019). During leachate extraction, each jar was quickly shaken by hand daily (2 times per day) for about 5 s, then returned to storage in the dark. The leaching process for RV, BF, MA, and FE was 24 hr, and for soils were 72 hr. After leaching, all sample solutions were filtered through 0.2 μm membrane filters (Pall Supor 200) into 4L acid-washed Nalgene bottles that contained 2L ultrapure water. Filtered leachates were stored at 4°C in the dark before inoculation within 24 hr.

2.4. BDOC Experimental Initiation and Setup

We defined the net change in DOC concentration from day 0 to day 28 as BDOC and %BDOC as the percentage of BDOC relative to initial DOC concentrations. To establish a generic riverine microbial community in each BDOC bottle, a 1% by volume microbial inoculation (Oldman River water filtered through pre-combusted 1.2 μm Whatman GF/D filters) was added into all sample solutions. This approach of inoculating 0.2 μm filtered leachates and river water with a small volume of a standardized microbial inoculum is similar to other work estimating relative rates of DOM biodegradation (Moran et al., 1999; Pinsonneault et al., 2016; Vaughn et al., 2023). We conducted parallel experiments using Oldman River ambient water samples with and without

microbial inoculation (OB and ON, respectively). The river water without inoculation (ON) was used as a negative control to explore potential effects of abiotic DOC transformations. Each inoculated solution and the negative river water control was quickly mixed by shaking the bottle right after inoculation, then day 0 subsamples were taken from each leachate sample right after shaking by filtering water through 0.2 μm syringe filters (Polyethersulfone, VWR) for later analyses. After all day 0 samples for each solution were taken, the 4L bottles were shaken again before equally dividing into three 1L acid washed amber bottle replicates and incubated in the dark at room temperature (21–23.5°C) for 28 days. Subsamples were then taken at day 2, 7, 14, 21, and 28 for analysis during the incubation.

2.5. DOC and Total Iron Concentrations

We measured the concentration of DOC in all subsamples using a Shimadzu TOC-L CPH high temperature catalytic oxidation total organic carbon analyzer calibrated with a six-point standard curve ($R^2 = 0.999$) based on the estimated concentration range of DOC in these samples. Each sample was acidified to pH 2 (1 μl 12 N HCl per 1 ml sample water) and run on the TOC analyzer following standard methods (Johnston et al., 2018; Zhou et al., 2023). We confirmed the effectiveness of the acidification step using pH paper, and checked to ensure samples remained acidified through time. We used acidified ultrapure lab water (pH = 2) as a blank. The concentration of each sample was determined by averaging 3 of the 7 injections with the lowest coefficient of variance (<0.02) and standard deviation ± 0.1. The final concentration of each sample was the average of these triplicates with some exceptions where we had unexplainable and extreme outlier concentrations that did not match other replicates (one LE replicate was removed from day 28, one RV replicate was removed from day 21, and one MA replicate was removed from day 14).

We measured iron concentrations to account for iron interference in optical measurements of DOM (Poulin et al., 2014). Total iron concentrations in water samples were determined using graphite furnace atomic absorption (GFAAS, GTA 120, Agilent Technologies, Santa Clara, California, USA). Instrument settings were set to a wavelength of 248.3 nm with 0.2 nm slit width, and background correction was enabled using a deuterium lamp. All samples were run according to the manufacturer's suggested settings within the SpectrAA software (Agilent Technologies, Santa Clara, California, USA), with the following modifications: a furnace burn-profile step was added (Step 9, temperature 2300°C, time 2.0 s, flow 0.3 L min^{-1} Ar) to eliminate carryover between samples and total sample volume was increased to 15 μL with a 10 μL sub-sample volume. A certified reference material, SLRS-6 (National Research Council of Canada) was run every 10 samples to evaluate accuracy, which was maintained above 90%. In instances where samples read outside of the calibration range, samples were auto-diluted using ultrapure water acidified to 1% using trace-metal grade 12 N nitric acid (CAS 7697-37-2) by a programmable auto-sampler (PD-120, Agilent Technologies, Santa Clara, California, USA). All samples and CRMs were run in duplicate. The detection limit for iron using this protocol was previously found to be 2 μg L^{-1} iron.

2.6. DOM Optical Properties

Fluorescence and absorbance measurements have been widely used to characterize the chemical composition of DOM (P. G. Coble, 2007; Dittmar & Stubbins, 2014; Fellman et al., 2010; Minor et al., 2014; Murphy et al., 2010). The absorption coefficient at 254nm (a_{254}) is commonly used as an indicator of colored DOM (CDOM) content, which is typically linearly related to DOC concentrations in ecosystems where colored aromatic materials dominate the DOM pool (Dittmar & Stubbins, 2014; Dobbs et al., 1972). The specific UV absorption coefficient at 254 nm ($SUVA_{254}$) is correlated to the aromaticity of (and typically the terrestrial contributions to) the DOM pool (Hansen et al., 2016; Helms et al., 2008; Weishaar et al., 2003). The spectral slope ratio (S_R) and fluorescence index (FI) are proxies for the relative molecular weight of DOM, with higher S_R and higher FI values indicating greater content of lower molecular weight DOM, which is commonly derived from more labile microbial or autochthonous sources (Fellman et al., 2010; Li & Hur, 2017; McKnight et al., 2001). The humification index (HIX) indicates the degree of humification or degradation of DOM, with more unsaturated DOM reflected in higher HIX values (Fellman et al., 2010; Ohno, 2002). Fluorescence peak intensities (i.e., the commonly used B, T, A, M, and C peaks) (P. G. Coble, 2007) can provide estimates of the contribution of different broad classes of DOM to the overall pool. The intensities of B and T peaks typically reflect protein-like DOM content while intensities of A, M, and C peaks indicate the contributions of humic-like DOM (P. G.

Coble, 2007; Fellman et al., 2010). The low cost and efficiency of optical measurements has enabled great advances in the study of aquatic DOM cycling.

Bulk DOM properties of ambient river water and leachates were measured using Biochrom Ultrospec 3100 pro UV-visible spectrophotometer and Shimadzu RF-6000 fluorometer, which were completed at room temperature using a 1 cm quartz cuvette and within 2 weeks of sub-sample collection. The absorbance spectra were measured from wavelengths 230–800 nm, at 1 nm intervals. Blank correction for absorbance spectra using ultrapure water was done automatically in the instrument software, and ultrapure water blanks were repeated every 10 samples for both absorbance and fluorescence spectra. Fluorescence spectra were measured in 5 nm intervals for excitation (between wavelengths of 230 and 500 nm) and in 2 nm intervals for emission (250–700 nm). During optical measurements, samples with higher DOC concentrations were diluted to <4 mg L^{-1}. Where absorbance or fluorescence were still over saturated, further dilutions were performed.

Absorbance and fluorescence spectra were processed using the StaRdom package (Pucher et al., 2019) in R (Dobbs et al., 1972; Helms et al., 2008; McKnight et al., 2001; Murphy et al., 2013; Ohno, 2002). Fluorescence spectra were inner-filter effect corrected then blank-corrected, and Raman normalized to Raman Units (R.U.) in R. We report the Napierian absorption coefficient at 254 nm (a_{254}, m^{-1}), spectral slope ratio (S_R; ratio of $S_{275–295}$ to $S_{350–400}$) (Helms et al., 2008), fluorescence index (FI, FI = em 450 nm/em 500 nm at ex = 370 nm) (McKnight et al., 2001), humification index (HIX) and fluorescence peaks B (ex = 270 nm, em = 310 nm), T (ex = 275 nm, em = 340 nm), A (ex = 260 nm, em = 380–410 nm), M (ex = 312 nm, em = 380–420 nm), and C (ex = 350 nm, em = 420–480 nm) (P. G. Coble, 2007). Individual peak intensities were reported as Raman normalized peaks in R.U. Each percent normalized peak was calculated by first dividing individual normalized peaks by maximum fluorescence (F_{max}), then dividing the normalized peak by the sum of the F_{max}-standardized peaks.

The specific ultraviolet absorbance at 254 nm ($SUVA_{254}$, L mg C^{-1} m^{-1}), a proxy for DOM aromaticity, was calculated using the decadic absorption coefficient (α_{254}, in m^{-1}) divided by the DOC concentration (mg L^{-1}), where α_{254} is calculated as:

$$\alpha_{254} = \frac{A}{l}$$

where A is the absorbance (unitless) and l is the path length in m.

To remove the interference of iron(III) in estimates of α_{254} and $SUVA_{254}$ (Poulin et al., 2014), an iron concentration-specific correction was applied to α_{254} using the following equation:

$$\alpha_{254\text{corrected}} = \alpha_{254\text{measured}} - (0.0653[\text{Iron(III)}] + 0.002)*100$$

for iron(III) concentrations between 0 and 1.5 mg L^{-1} (Poulin et al., 2014), where α_{254} is the decadic absorption coefficient (m^{-1}) for our study and multiplying by 100 converts the correction factor from cm^{-1} (Poulin et al., 2014) to m^{-1}. Iron(III) concentrations are in mg L^{-1}. We assumed that iron(III) concentrations were equivalent to the total iron concentrations, given that iron(III) is generally the dominant form in oxic alkaline waters (Namieśnik & Rabajczyk, 2015). Overall, the Fe:DOC ratio in both river samples and leachates was low (<0.02 mg_{Fe} $mg_C{}^{-1}$, see Results: Tables 1 and 2), suggesting little impact of iron on a_{254} or $SUVA_{254}$ (Logozzo et al., 2022).

2.7. DOC Decay Rate and Half-Life Calculations

Changes in DOC concentration during BDOC experiments with river water and the individual leachate DOM sources were calculated following Catalán et al. (2016) and Guillemette and del Giorgio (2011), as described in Zhou et al. (2023). Briefly, decay coefficients (k) for incubations using leachates and filtered river water were calculated as $k = \ln(t/i)/T$, where i is the average DOC concentration based on triplicate samples at day 0 of an incubation, and t is the average concentration on day T. Half-life ($t_{1/2}$) was calculated as $t_{1/2} = \ln(2)/k$. For each incubation, k was calculated in R version 4. 1. 2 (R Core Team, 2021) using the *dplyr* package for data manipulations.

Journal of Geophysical Research: Biogeosciences 10.1029/2023JG007831

Table 1
Summary of General and Optical Properties for River Samples Across Seasons

Sample	Time of sampling	Mean discharge ($m^3\ s^{-1}$)	DOC ($mg\ L^{-1}$)	Iron ($mg\ L^{-1}$)	a_{254} (m^{-1})	$SUVA_{254}$ ($L\ mg\ C^{-1}\ m^{-1}$)	S_R	Intensity of Raman normalized peaks (R.U.)					FI	HIX
								B peak	T peak	A peak	M peak	C peak		
OMW-Sept	17 September 2021	23.2 (0.7)	1.75 (0.02)	0.002	8.4 (0.1)	1.98 (0.05)	1.1 (0.3)	0.14 (0.00)	0.09 (0.00)	0.10 (0.00)	0.10 (0.00)	0.06 (0.00)	1.34 (0.02)	0.46 (0.00)
OMW-Mar	07 March 2022	NA	1.33 (0.03)	0.005	6.5 (0.1)	1.95 (0.06)	0.5 (0.1)	0.13 (0.00)	0.06 (0.00)	0.08 (0.00)	0.09 (0.00)	0.06 (0.00)	1.40 (0.01)	0.42 (0.00)
OMW-Jun-L	01 June 2022	23.5 (0.2)	2.15 (0.02)	0.022	9.9 (0.5)	1.84 (0.09)	1.3 (0.2)	0.07 (0.00)	0.07 (0.00)	0.09 (0.00)	0.11 (0.00)	0.08 (0.00)	1.33 (0.01)	0.62 (0.01)
OMW-Jun-H	15 June 2022	361 (12)	2.11 (0.03)	L	11.8 (0.4)	2.34 (0.04)	1.1 (0.2)	0.10 (0.00)	0.13 (0.04)	0.14 (0.00)	0.17 (0.00)	0.13 (0.00)	1.39 (0.01)	0.64 (0.03)

Note. NA indicates data not available. L indicates the iron concentration was below detection limit, which is $<2\ \mu g\ L^{-1}$. Mean of results are included and standard deviation is shown (in parentheses).

Table 2
Summary of General and Optical Properties for Leachate Samples at Day 0

Source type	DOC (mg L^{-1})	Iron (mg L^{-1})	a_{254} (m^{-1})	$SUVA_{254}$ (L mg C^{-1} m^{-1})	S_R	Raman normalized peak intensity (R.U.)					FI	HIX
						B peak	T peak	A peak	M peak	C peak		
LE	101 (1)	L	146 (2)	0.63 (0.01)	0.8 (0.1)	27.58 (1.39)	10.05 (0.64)	1.58 (0.24)	6.28 (0.22)	0.53 (0.05)	1.73 (0.13)	0.01 (0.02)
RV	88.4 (0.6)	L	190 (4)	0.93 (0.02)	0.6 (0.0)	10.17 (0.06)	6.75 (0.11)	1.59 (0.03)	4.70 (0.05)	1.08 (0.01)	1.73 (0.02)	0.13 (0.00)
GR	97.4 (1.7)	0.007	92 (0)	0.41 (0.01)	0.4 (0.0)	3.88 (0.05)	5.51 (0.04)	1.42 (0.05)	1.53 (0.02)	0.68 (0.00)	1.74 (0.07)	0.19 (0.00)
TS	3.08 (0.05)	0.006	18 (0)	2.40 (0.04)	0.9 (0.1)	0.17 (0.01)	0.27 (0.01)	0.34 (0.00)	0.43 (0.01)	0.30 (0.00)	1.32 (0.01)	0.75 (0.00)
MS	13.2 (0.3)	0.11	79 (2)	2.53 (0.08)	0.8 (0.1)	0.74 (0.03)	0.63 (0.04)	1.21 (0.02)	1.55 (0.02)	1.07 (0.01)	1.27 (0.00)	0.79 (0.01)
RS	1.37 (0.03)	L	9.3 (0.1)	2.79 (0.09)	0.7 (0.1)	0.11 (0.00)	0.10 (0.01)	0.23 (0.00)	0.25 (0.01)	0.18 (0.00)	1.37 (0.02)	0.66 (0.00)
FE	3.57 (0.11)	L	5.4 (0.4)	0.60 (0.05)	0.4 (0.4)	0.54 (0.00)	0.63 (0.01)	0.11 (0.00)	0.08 (0.00)	0.09 (0.00)	1.90 (0.04)	0.26 (0.01)
MA	19.7 (0.08)	0.013	25 (1)	0.53 (0.02)	1.3 (0.3)	1.26 (0.02)	0.71 (0.01)	0.17 (0.02)	0.15 (0.01)	0.15 (0.01)	1.41 (0.05)	0.26 (0.02)
BF	8.53 (0.01)	0.003	9.5 (0.5)	0.46 (0.03)	0.8 (0.1)	1.21 (0.01)	1.13 (0.03)	0.36 (0.01)	0.34 (0.00)	0.23 (0.00)	2.16 (0.07)	0.35 (0.00)

Note. L indicates the concentration of iron is below detection limit, which is <2 μg L^{-1}. Mean of results are included and standard deviation is shown (in parentheses).

2.8. Statistical Analyses

Principal component analysis (PCA) was performed in R using the *vegan* package. The percent BDOC (% BDOC), initial DOC concentrations, *k*, and optical parameters for all leachate and river samples from initial day (T0) BDOCs were averaged among triplicates in the PCA to determine the relationship between river and leachate samples. All parameters were scaled and mean-centered. The linear regression relationship between $\log_{10}(t_{1/2})$, % normalized peaks, and other optical parameters was calculated using the lm() function in base R. The analysis of variance (ANOVA) with Tukey's honest significant difference *post hoc* tests (Kao & Green, 2008) (*Tukey_hsd* function) was performed to compare initial DOC concentration and selected optical parameters between river samples. In some cases, (e.g., for $SUVA_{254}$) all replicates had identical values and we were unable to conduct statistical analyses with these individual samples, so they were excluded from statistical analyses but are presented graphically. Paired *t*-tests were used for determining the significant difference of net change in normalized peak intensities for all leachate sources except leaves, riparian vegetation, and macrophyte and river samples.

3. Results

3.1. River DOC Concentrations

The DOC concentration in river water (i.e., the initial samples for ambient river water BDOC) ranged from 1.33 ± 0.03 mg L^{-1} (mean ± standard deviation) to 2.15 ± 0.02 mg L^{-1} (Figure 2a, Table 1). The highest DOC concentrations occurred during the June pre-flood period (i.e., pre-spring freshet), and the lowest occurred in March (winter). There was no significant change in DOC concentrations from spring baseflow to the freshet ($p = 0.28$).

3.2. River DOM Composition

The five fluorescence peak intensities were similar during the three baseflow sampling periods and increased during the spring freshet (except peak B) (Figure 2b, Table 1). For peak B, the Raman normalized intensity (Figure 2b) was higher in September (0.14 R.U.) and March (0.13 R.U.) and lowest during June pre-flood (0.07 R.U.), but moderate during the June freshet (0.10 R.U.). Intensities for the other fluorescence peaks from September, March, and June (pre-flood) ranged little, from 0.06 to 0.09 R.U. (peak T), 0.08 to 0.10 R.U. (peak A), 0.09 to 0.11 R.U. (peak M), and 0.06 to 0.08 R.U. (peak C) (Figure 2b). Between June pre-flood and flood periods, peak intensities increased by 43% (B), 86% (T), 67% (A), 55% (M), and 63% (C) (not shown). Considering Raman normalized DOM fluorescence intensity as a percentage of F_{max} (Figure 2c), peak contributions were consistent between autumn and winter (September and March), with protein-like DOM (peaks T and B) contributing 46.3%–47.3% to F_{max}. Peaks M, A, and C contributed a summed ∼53% of the remaining F_{max} in autumn and winter (Figure 2c). There was a shift in relative peak contributions to F_{max} in spring (June), with protein-like DOM (B and T peaks) contributing only 33.1%–34.5% to F_{max}. In June for both the pre-flood and flood periods, peaks A,

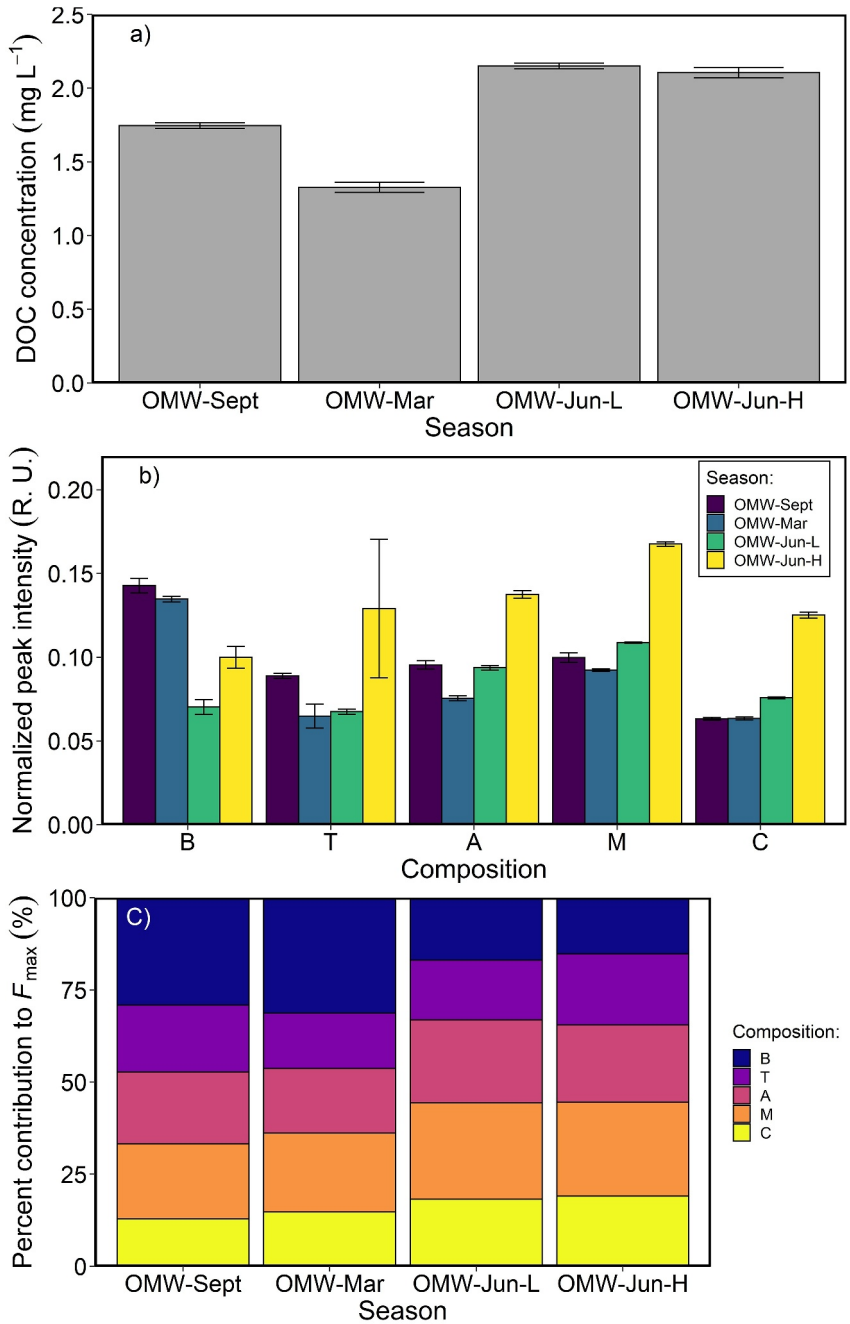

Figure 2. Initial (a) dissolved organic carbon concentration, and Raman normalized fluorescent peak (b) intensities and (c) percent contribution to F_{max}, for the Oldman River across seasons: September (OMW-Sept), March (OMW-Mar), June low flow (OMW-Jun-L), and June Spring flood (OMW-Jun-H). Each bar represents the average of triplicate measurements, where error bars are ±1 standard deviation.

M, and C each contributed a relatively larger fraction than in autumn and winter and the sum of these peaks contributed the bulk of F_{max}. We saw little change in peak intensities in samples from June pre-flood and flood periods (Figure 2c).

The absorbance properties of river samples were comparatively inconsistent in pattern across sampling periods (Table 1). Values of $SUVA_{254}$ were <2 for the three first sampling periods, then increased to 2.34 L mg C^{-1} m^{-1} during the June flood. The FI was consistently terrestrial-like but ranged between seasons from 1.33 to 1.40 (ANOVA, $p < 0.001$; Table 1). We observed significant differences between values in March and June before the

freshet (1.40 vs. 1.33; Tukey's post hoc: $p < 0.002$). HIX showed a smaller range in values, from 0.46 to 0.64, with only a marginal difference between September and March (Tukey's post hoc, $p = 0.07$) and no significant difference between June pre-flood and flood (Tukey's post hoc, $p = 0.62$; Table 1).

3.3. Initial DOC Concentration and DOM Composition in Leachates

The extractable DOC content varied by over two orders of magnitude among endmember leachates. The concentration of DOC was greatest in terrestrial vegetation leachates (88.4–101 mg L^{-1}). In soil and aquatic source leachates, DOC concentrations were all lower than for vegetation, but varied considerably (Figure 3a, Table 2). Of the three types of river valley soils, the highest DOC concentration was found in leachates from the midpoint soil (13.2 ± 0.3 mg L^{-1}) and lowest in the riparian soil (1.37 ± 0.03 mg L^{-1}). Among the three aquatic end members, the highest DOC concentration was found in leachates from macrophytes (19.70 ± 0.08 mg L^{-1}) and lowest from FE (3.57 ± 0.11 mg L^{-1}) (Figure 3a, Table 2).

The composition of leachate-derived DOM varied considerably between soils, terrestrial vegetation, and aquatic sources. The three vegetation leachates (LE, RV, and GR) had the highest peak intensities for all fluorescent peaks. Among terrestrial vegetation leachates, LE showed the highest B and T peak intensities (27.58 and 10.05 R.U.) followed by RV (10.17 and 6.75 R.U.) and GR (3.88 and 5.51 R.U., respectively). Leachates from aquatic sources (MA, FE, BF) showed the next highest peak intensities for B and T, but lower peak intensities for A, M, and C compared to soil leachates (Figure 3b, Table 2). For the soil end member leachates, the intensities for peaks B and T were relatively low (from 0.11 to 0.74 and 0.10–0.63 R.U., respectively). Similar to patterns for DOC concentration, leachates from MS showed higher peak intensities for all components compared to TS and RS (Figure 3b, Table 2). The ratio of A:T was highest in soils (2.19, 1.91, and 1.24 for RS, MS, and TS, respectively), while the other leachates had low ratios, within the range of 0.16–0.26 (data not shown).

When scaled as a percentage of Raman normalized peak contributions to F_{max} (Figure 3c), the soil leachates had the most unique DOM composition, compared to vegetation and aquatic end member leachates. For soil leachates, the summed percent contribution of peaks B and T was low (24.3% ± 1.3% to 29.3% ± 0.5%), whereas percent contribution of peaks A, M, and C were relatively large (70.7% ± 0.2% to 75.7% ± 0.9%) compared to terrestrial vegetation and aquatic sources. In contrast, vegetation and aquatic end member leachates were dominated by peaks B and T (69.7% ± 0.5% to 81.8% ± 0.3%; Figure 3c). These leachates had low aromaticity and potentially higher bioavailability ($SUVA_{254}$: 0.41–0.93 L mg C^{-1} m^{-1}; HIX: 0.01 to 0.35; and FI: 1.41 to 2.16; Table 2). Soil leachates had higher aromaticity, ranging from 2.40 to 2.79 L mg C^{-1} m^{-1} for $SUVA_{254}$, as well as higher HIX (0.66–0.79), and lower FI (1.27–1.37) values (Table 2).

3.4. BDOC Patterns for Leachates and River Water

Throughout the Oldman River valley, individual DOM endmember leachates had a wide range in bioavailability and turnover but were all greater than that of river water DOM (Figure 4 and Figure S1 in Supporting Information S1). Total BDOC values were highest for terrestrial vegetation leachates (74.6 ± 0.6 to 84.6 ± 1.8 mg L^{-1}). Among remaining endmember leachate incubations, BDOC varied from as low as 0.33 ± 0.04 mg L^{-1} for riparian soil up to 13.3 ± 0.4 mg L^{-1} for macrophytes. The river water incubations consistently had the lowest BDOC concentrations (0 to 0.29 ± 0.02 mg L^{-1}). Similarly, the percent BDOC was also highest in terrestrial vegetation leachate incubations (83.8%–86.8%) and lowest for the river water incubations (0%–16.6%, Figure 4b). For soils, top of river valley soil and mid point soil showed a similar percent BDOC (53.7% ± 1.7% and 56.7% ± 2.8%, respectively) while riparian soil was only 23.9% ± 3.1%. For aquatic sources, the percent BDOC varied widely for each end member, increasing from FE (49.9% ± 3.7%) to macrophytes and biofilm (67.4% ± 2.0% and 80.0% ± 1.0%, respectively). For river water BDOC, values were lowest in spring (0%–3.2% ± 3.6%) compared to autumn and winter (16.6% ± 1.2% and 8.5% ± 2.6%, respectively) (Figure 4b). The average percent BDOC for river water across the year was 7.1% ± 2.1%. The DOC decay coefficient (k) was highest for all terrestrial vegetation leachates (0.057–0.074 day^{-1}) and lowest for river water (0.002–0.006 day^{-1}, Figure 4c and Figure S1 in Supporting Information S1). Values of k decreased for aquatic end member leachates for biofilm, macrophytes, and FE, respectively (0.060, 0.039, and 0.025 day^{-1}). For terrestrial leachates, values of k decreased from top to riparian soil leachates (0.027, 0.022, and 0.009 day^{-1}) and from smaller vegetation (grass; 0.074 day^{-1}) to larger vegetation (Cottonwood trees; 0.057 day^{-1}) (Figure 4c and Figure S1 in Supporting Information S1). Over the course of each incubation, most leachates typically underwent

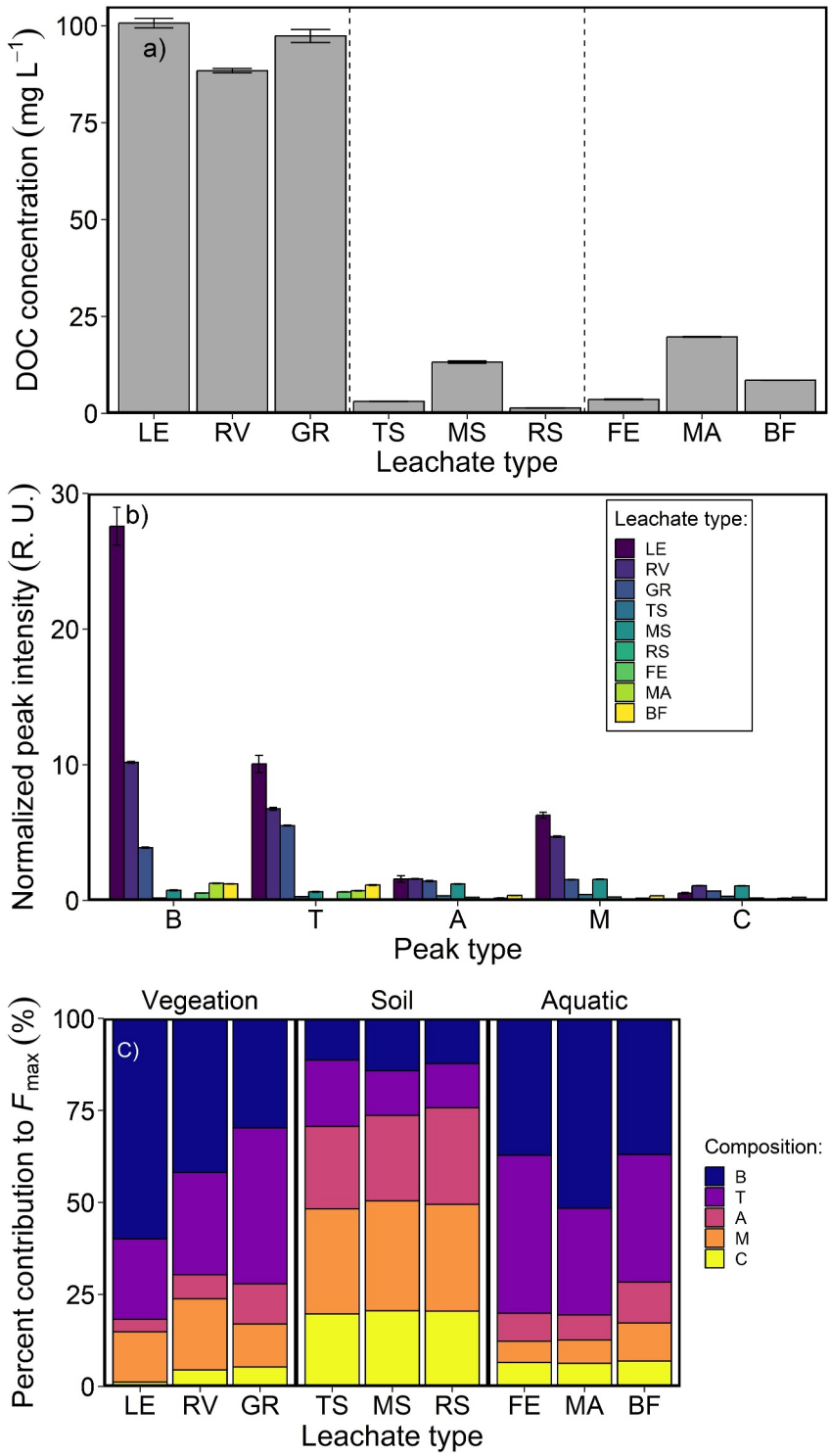

Figure 3. Initial (a) dissolved organic carbon concentration, and Raman normalized fluorescent peak (b) intensities and (c) percent contribution to F_{max} for all leachates, including 3 vegetation types (LE, RV, and GR for leaf, riparian vegetation, and grass leachates, respectively), 3 surface soil types (RS, MS, and TS for leachates from soils at riparian, mid-valley, and top of valley locations, respectively), and 3 aquatic dissolved organic matter (DOM) sources (FE, MA, and BF, for fish excretion DOM, and macrophyte and biofilm leachates, respectively). Each bar represents the average of triplicate measurements, where error bars are ±1 standard deviation.

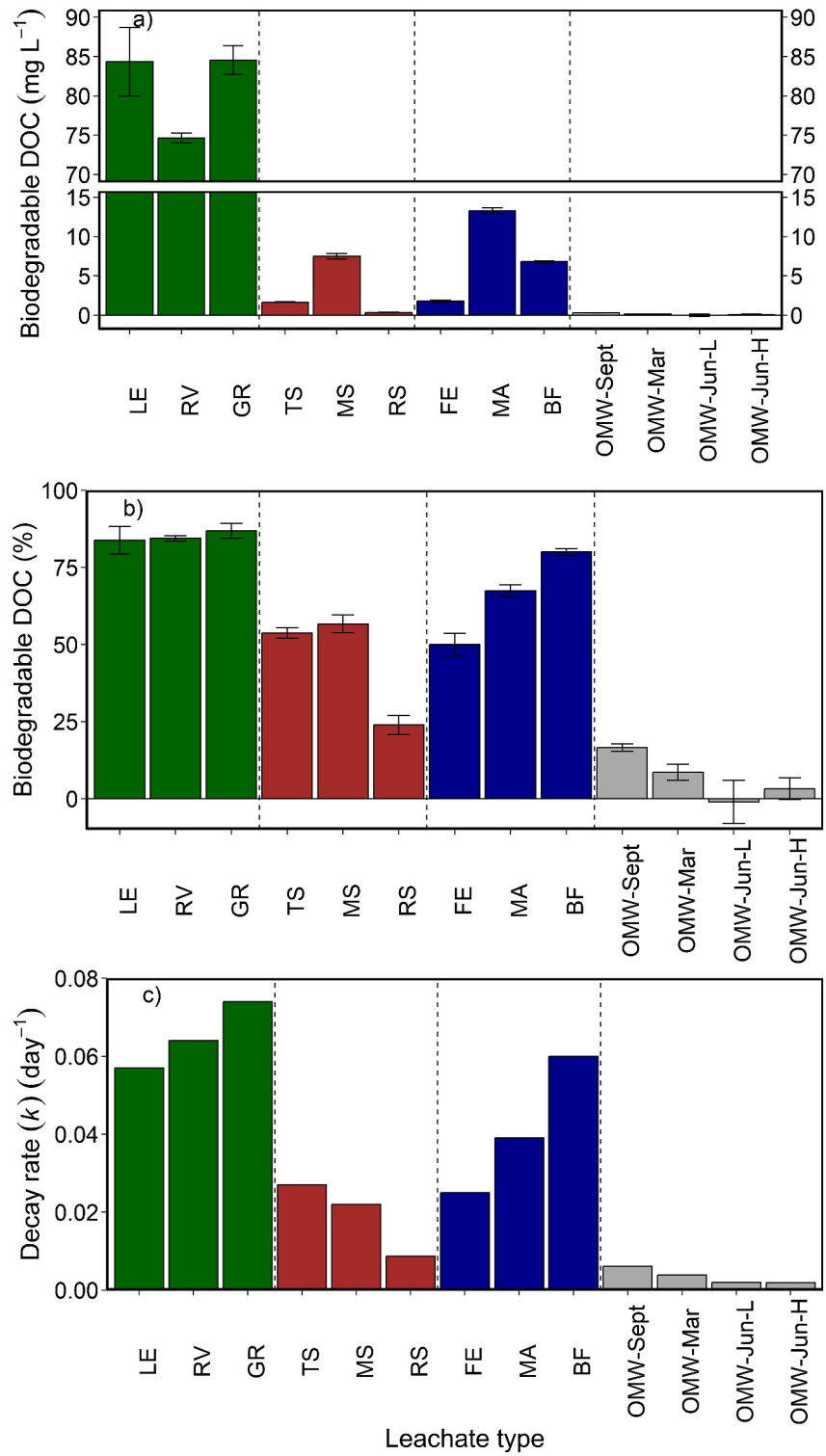

Figure 4. (a) Net change of dissolved organic carbon (DOC) from day 0 to 28, or biodegradable dissolved organic carbon (BDOC), (b) percent biodegradable DOC (%BDOC), and (c) decay rate (k) for all leachate sources and river samples across seasons: September 2021, March 2022, June 2022 low flow, and June 2022 high flow (15 June 2022). Error bars represent ±1 standard deviation.

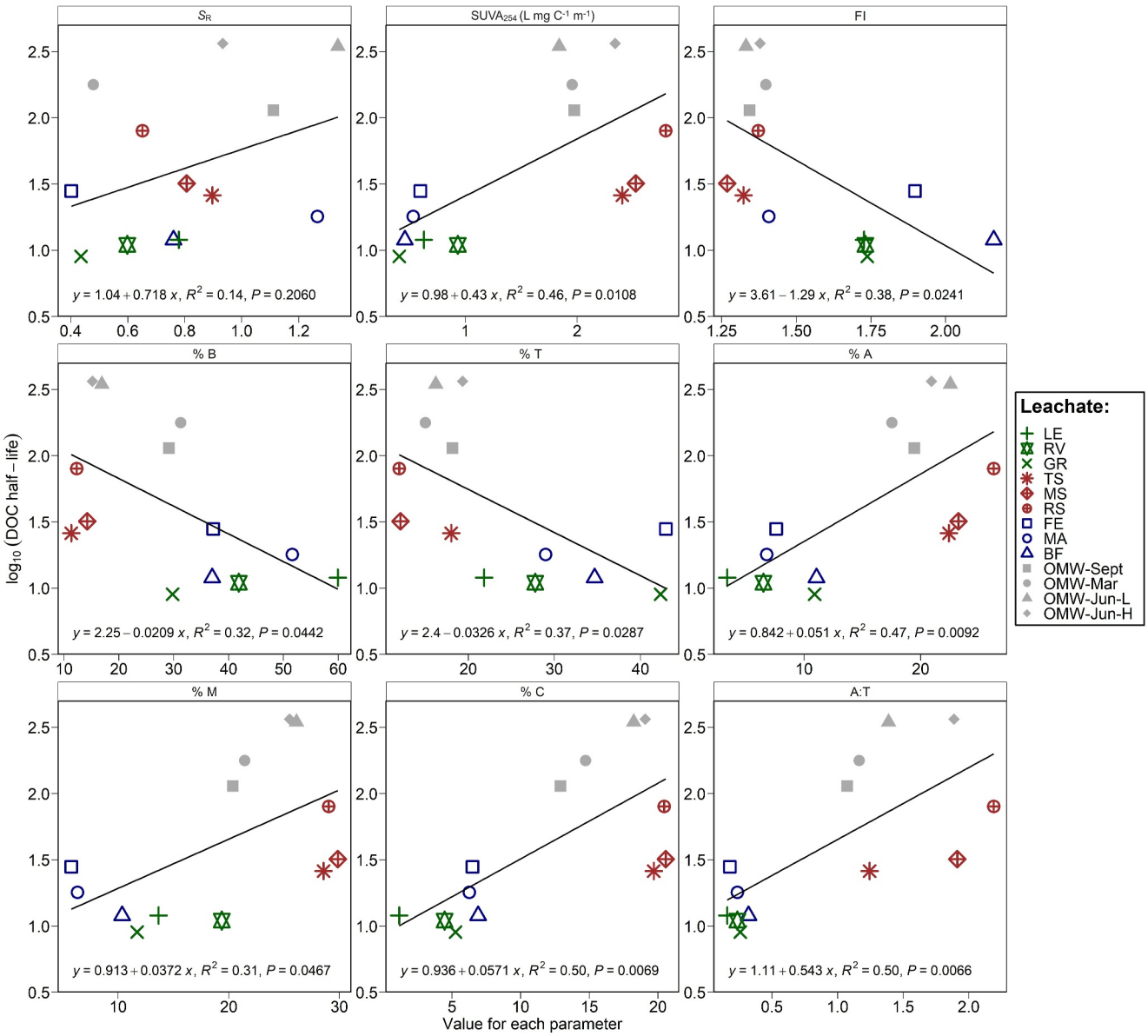

Figure 5. Relationship between $\log_{10}$(half-life) to bulk optical parameters including individual absorbance metrics (S_R, $SUVA_{254}$, and fluorescence index) and the percent individual peak (B, T, A, M, C) contribution to F_{max}.

a net decrease in DOC concentration, fluorescent peak intensities, S_R and FI values, and a net increase in $SUVA_{254}$, HIX, and A:T peak ratios (Table S1 in Supporting Information S1). The exception was LE, which showed a large increase in values for A, M, and C peaks (2.4–3.8 times).

The chemical properties of leachates (Figure 5) and the total amount of DOC available (Figure 6) were correlated to different degrees with their bioavailability and their potential residence time in the aquatic environment, as summarized by the log-transformed half-life of DOC. Overall, of the measurements of DOM chemical composition, the best predictors of DOC half-life in incubations were values of the A:T ratio ($R^2 = 0.50$, $p = 0.006$), the % contribution of C peak ($R^2 = 0.50$, $p = 0.0069$), and A peak to F_{max} ($R^2 = 0.47$, $p = 0.0092$). The weakest predictors were S_R ($R^2 = 0.14$, $p = 0.21$), and the % contribution of M peak ($R^2 = 0.31$, $p = 0.047$), and B peak to F_{max} ($R^2 = 0.32$, $p = 0.044$). At the same time, the log-transformed concentration of DOC was strongly positively related to %BDOC (Figure 6a; $R^2 = 0.76$) and values of k (Figure 6b; $R^2 = 0.81$). A weaker relationship was present between concentrations of DOC and half-life of the pool (Figure 6c; $R^2 = 0.65$).

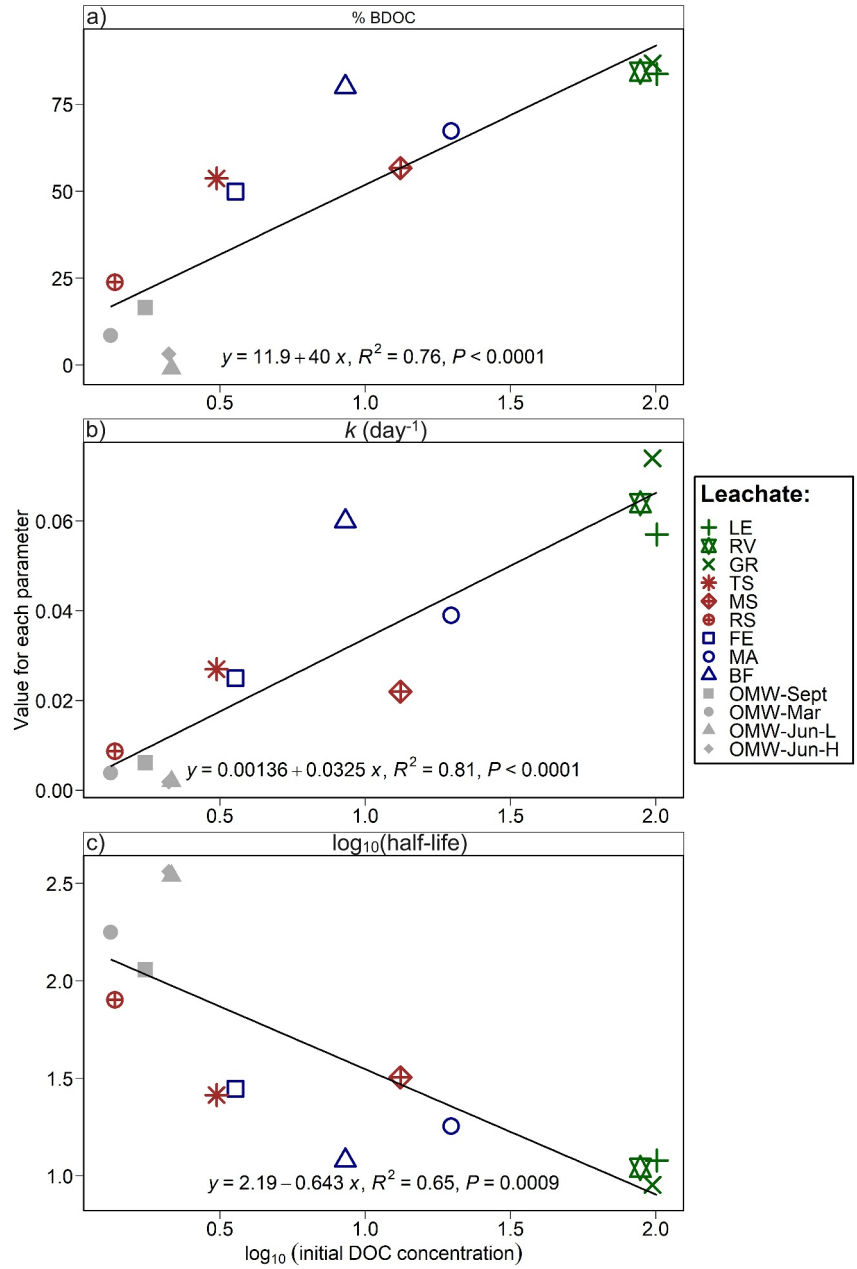

Figure 6. Relationship between $\log_{10}$ values of initial dissolved organic carbon (DOC) concentration in biodegradable dissolved organic carbon (BDOC) incubations, versus metrics of DOC mineralization including (a) %BDOC, (b) the DOC decay coefficient, and (c) $\log_{10}$(DOC half-life).

3.5. PCA for Leachate and River Samples

The PCA captured a total of 81.4% of the variation between DOM sources using parameters as shown in Figure 7 (Table S2 in Supporting Information S1) and showed no major differences between river samples across seasons and during the spring flood. Principal component 1 (PC1) explained 68.8% of the variation in the data set for initial leachate and river samples, and was positively related to $SUVA_{254}$, A:T peak ratios, and the ratios of A, M, and C peaks to F_{max}, which collectively reflect more aromatic and possibly less bioavailable DOM pools. The more negative loadings on PC1 were related to higher leachable DOC concentrations, the ratios of B and T peaks to F_{max}, and larger FI values (Figure 7, Table S2 in Supporting Information S1). Leachate samples of terrestrial vegetation and aquatic sources tended to load more negatively on PC1, while soil leachate and water samples

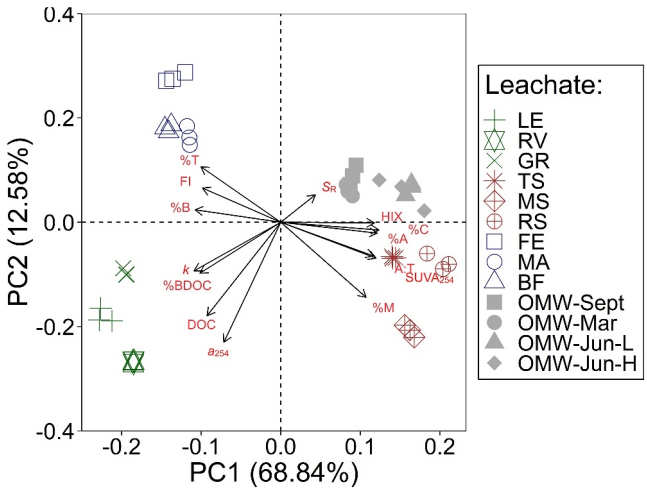

Figure 7. Principal components analysis of %biodegradable dissolved organic carbon, initial dissolved organic carbon concentration, and optical parameters for principal components 1 and 2 (PC1 and PC2). Symbols represent different leachate sources and river water from different seasons, and the parameters used for Principal component analysis are shown in red color. Loadings are summarized in Table S2 in Supporting Information S1.

loaded more positively on axis 1. PC2 explained 12.6% of the variation within the data set and was most strongly related to UV absorbance (a_{254}), likely reflecting the quantity of DOM in samples, given that DOC concentrations and absorbance values were positively correlated (Pearson correlation of $\log_{10}$ transformed values: $r^2 = 0.76$, $p = 0.001$) and had similar loadings on PC1 and PC2. Not surprisingly for BDOC incubations, the values of k and %BDOC were most strongly related to variables with negative loadings on PC1 and PC2, with samples that had more leachable DOC, higher contributions of B and T peaks, lower $SUVA_{254}$, and lower A:T peak ratios having faster turnover of the DOC pool in incubations (Figure 7, Table S2 in Supporting Information S1).

4. Discussion

The DOM in the Oldman River consistently resembled terrestrial soil leachates in composition, and secondarily autochthonous DOM sources (Figure 7), even though we found a wide range in composition, leachable DOC content, and bioavailability of potential DOM sources among the various end members throughout the river valley (Figures 4–6). River DOM also had consistently low bioavailability relative to leachates. At a finer temporal scale, smaller seasonal differences in DOM cycling reflect the dynamic features of this river ecosystem. The river had relatively consistent DOC concentrations that varied by ~1 mg L^{-1} throughout the year (Figure 2a), despite discharge varying >15-fold from baseflow to flood periods. During spring (Figure 2c), the river's DOM pool consisted of material that was more characteristic of soil-like DOM endmembers that were less bioavailable, whereas in autumn (September) and winter (March) the DOM pool shifted modestly to resemble autochthonous-like end members (fish, macrophyte, and biofilm sources) that were more bioavailable (Figures 2c, 3c, and 5). Overall, not only is the mainstem Oldman River a relatively small exporter of DOM (in terms of catchment yield) when compared to other river systems (Johnston, Gunawardana, et al., 2022), it may also support limited internal processing and turnover of DOM under current hydroclimatic conditions, at least at the mainstem location sampled here. It is likely that upstream impoundment and flow regulation (e.g., Oliver et al., 2016) play an important role in stabilizing the seasonal variability in DOM composition and content in the river mainstem.

4.1. Limited DOM Biodegradability in the Oldman River

We found consistently low DOC concentrations and low DOM biodegradability throughout the year in the mainstem of the Oldman River, though there were clear seasonal differences in both parameters. The annual average %BDOC for the Oldman River (7.1% ± 2.1%; Figure 2) was on the low end of the range of measured values for global rivers (0.1%–72.2%, average of 16.4%) (F. Liu & Wang, 2022), while the average decay coefficient (0.0035 ± 0.002 day^{-1}; $n = 4$) is similar to the mean for rivers globally (0.0034 ± 0.0219 day^{-1}) (Catalán et al., 2016), but was on the high end of decay rates from a heavily impounded North American semi-arid river (ranging from 0.0014 to 0.0036 day^{-1}) (Ulseth & Hall, 2015). More broadly, our findings align with the lower end of median values from incubations reported for global aquatic habitats, which tend to decrease in %BDOC along the aquatic continuum from >20% in lakes to <~5% in the open ocean (LaBrie et al., 2020). Yet for each habitat type there exists a wide range in values and sites that have low %BDOC (LaBrie et al., 2020; F. Liu & Wang, 2022), so in this regard the low values for Oldman River %BDOC are not anomalous. Instead, upstream impoundments (Figure 1) that have lengthened hydrologic residence times in the downstream river mainstem (Rock & Mayer, 2007) have likely stabilized and restricted the extent of microbial DOM processing in the Oldman River downstream of the reservoir (Oliver et al., 2016). Reservoir construction and longer water residence times enhance riverine DOM removal and replacement (Johnston, Gunawardana, et al., 2022; Maavara et al., 2020; Ulseth & Hall, 2015). As shown by Ulseth and Hall (2015), the bioavailability of DOM decreased below large reservoirs in arid rivers of the U.S., due to fast turnover of autochthonous DOM and higher photooxidation of terrestrial DOM in the reservoirs. Also, retention in reservoirs can limit downstream nutrient availability and restrict heterotrophic DOM processing (Maavara et al., 2020; Wang et al., 2018). While extreme

hydrologic regulation has likely modified DOM cycling in the mainstem of the Oldman River, follow up work is needed to confirm these impacts.

The low bioavailability of DOM in incubations of river water suggests limited DOM microbial turnover may occur in the downstream habitat of the Oldman River. Our results are conservative, since our incubations only used suspended microbes and do not capture particle-bound microbial community metabolism, nor sediment heterotrophic processes (a hotspot for DOC transformation; Kelso et al., 2020; Risse-Buhl et al., 2012) or photo-oxidation of aromatic DOM. Further, our incubations were not persistently shaken to simulate advective or turbulent mixing that enhances the supply of fresh DOM and nutrients to microbes to sustain elevated rates of respiration (Ward et al., 2018). Therefore, the rates of microbial respiration in these incubations would be further considered conservative. Collectively, these processes would enhance DOM turnover. However, $SUVA_{254}$ values for the Oldman River (1.84–2.34 L mg C^{-1} m^{-1}, Table 1) were low compared to other systems (e.g., 1.3–4.7 L mg C^{-1} m^{-1} for a temperate river (Hanley et al., 2013), 2.2–3.4 L mg C^{-1} m^{-1} for Arctic rivers (O'Donnell et al., 2016), and 1.68–4.79 L mg C^{-1} m^{-1} globally for freshwater systems (Massicotte et al., 2017)). Therefore, DOM in the Oldman River downstream of the reservoir is likely less photo-reactive (Lapierre & del Giorgio, 2014), and not subject to much enhanced DOM biodegradation via photo-priming mechanisms (Logozzo et al., 2021; Moran & Covert, 2003). While the rates of microbial DOC removal that we report may be an underestimate of ecosystem heterotrophic processes, they provide general context on DOM turnover in this system (Kelso et al., 2020), and are an important platform to guide future research into ecosystem-scale DOM cycling in the Oldman River and similar ecosystems.

4.2. Modest Seasonal Changes in DOM Composition and Processing do Not Track Export

While the annual average export rate of DOC is low compared to other rivers (7.2 ± 4.5 Gg yr^{-1}, Johnston, Gunawardana, et al., 2022), we observed large seasonality in discharge and likely DOC export that is independent of patterns of DOM composition, concentration, or bioavailability. While discharge increased >15-fold from autumn to the spring flood (freshet) period, DOC concentrations changed little across season or discharge (Figure 1c, Table 1). Given the increase in discharge without changes in DOC concentration, we qualitatively infer that DOC lateral flux would have increased greatly during the freshet, without a corresponding change in DOM composition. This trend is consistent with other large regulated rivers (Oliver et al., 2016; Ulseth & Hall, 2015) and temperate mainstem rivers that demonstrate chemostasis as a result of DOM source-switching (Hosen et al., 2020). At high flow, the contribution of allochthonous DOM can increase with greater lateral export from terrestrial landscapes (Hosen et al., 2020; Logozzo et al., 2023). At low flow, as allochthonous DOM contributions decrease, autochthonous production of DOM often increases (Hosen et al., 2020; Logozzo et al., 2023; Oliver et al., 2016), as can the relative contributions from groundwater rich in less-aromatic DOM (Fellman et al., 2014; Hosen et al., 2021), and other processed allochthonous sources (Barnes et al., 2018). Thus, while these are largely qualitative assessments that we cannot validate with a quantitative mass balance (given the lack of suitable data), it does make sense that internally sourced DOM should reach a peak in contribution to the river mainstem when temperatures are warmest, when autochthonous food web growth and biomass in the Oldman River is known to be elevated in late summer and early autumn (Culp & Davies, 1982), and when connectivity between terrestrial DOM sources (e.g., surface soils) is lower due to lower river flow (Barnes et al., 2018; Oliver et al., 2016).

Moderate seasonal changes in the DOM composition of river water (Figures 2 and 7, Table 1) indicate that shifts in contributions from distinct sources may result in less seasonal variation in DOM composition. We did observe a clear ~0.6 L mg^{-1} m^{-1} increase in $SUVA_{254}$ during the spring freshet (Table 1), indicative of greater terrestrial connectivity and inputs of aromatic, soil-derived DOM (Hansen et al., 2016). Yet the relative contribution of distinct FDOM peaks changed little in the spring prior to (low flow) and during the freshet (high flow) (Figure 2c), suggesting that compositional shifts in the DOM pool during spring may have initiated prior to peak discharge. There was a clear shift from spring to summer and autumn in FDOM composition, with B peak contributions dominating in autumn, supporting the idea that greater relative inputs of autochthonous and more processed (or groundwater) allochthonous sources sustain DOM concentrations (detailed above). In line with this, the DOM pool shifted in composition in autumn and winter (Figures 2c and 7) toward DOM endmembers of autochthonous origin (macrophytes, biofilm, fish excretory products) (Figures 3c and 7). Such autochthonous DOM supply could be both local in the river and transported downstream from the large impoundments above our sampling location (Figure 1, Oliver et al., 2016). The PCA summarizing DOM composition, total DOC leachability, and

bioavailability showed river samples resembled a mixture of soil leachate (PC1, 68.8%) and autochthonous leachate DOM (PC2, 12.6%; Figure 7, Table S2 in Supporting Information S1). The dominance of soil sources to river DOM aligns with earlier studies indicating riparian and groundwater inputs supplied the bulk of river DOM in small creeks in Hűttenberg, Germany (Seifert et al., 2016). Further, previous work has also shown that fresh plant and algal-derived DOM is highly labile and does not persist in river reaches extending below impoundments (e.g., Oliver et al., 2016), so fresh autochthonous endmembers are not expected to comprise a large fraction of DOM in most aquatic environments (Hansen et al., 2016). Impoundment and reservoir construction enhances the production and downstream export of phytoplankton-derived DOM (e.g., Oliver et al., 2016) and OM production in dam tailwaters (Ulseth & Hall, 2015). While we cannot currently identify the location of autochthonous DOM production in the Oldman River, internal production clearly plays an important, but secondary role in the DOM cycle of this river, and possibly other large rivers in the region.

Seasonal shifts in DOM composition had clear implications for the functioning of the food web due to shifts in microbial processing capacities of the DOM pool, which regulates the flow of energy and nutrients from the DOM pool to the base of the food web (Findlay & Sinsabaugh, 2003). The percent BDOC values were highest in autumn and lowest in the spring, including during the freshet (Figures 4b and 4c). Similar to other work in a northern temperate watershed in the U.S. (A. A. Coble et al., 2016) and the Costal Plain of Maryland (Hosen et al., 2014), our study also showed that the higher percent BDOC in the autumn scaled positively with relative contributions of protein-like DOM (Figures 5 and 7). This stresses how periods of low flow, when transit time is long, are associated with some of the most bioavailable DOM, apparently linked to elevated autochthonous inputs of biolabile DOM (discussed above). Of interest, we observed variation in %BDOC between September (16.6%) and March (8.5%) (Figures 4b and 4c), despite the similar CDOM composition and aromaticity in these periods (Figure 2c, Table 2). This difference is consistent with previous work (A. A. Coble et al., 2016) and suggests that additional parameters control the bioavailability of river DOM beyond chemical composition alone, or that non-colored DOM may variably influence BDOC between these periods. Thus, follow up work on the Oldman River can refine our understanding of DOM cycling by potentially considering other known drivers such as microbial community compositional shifts across seasons (Hullar et al., 2006), and water quality parameters including availability of inorganic nutrients to support microbial DOM processing (F. Liu & Wang, 2022; Shousha et al., 2022).

Few studies have considered winter DOM composition and processing, especially in Canadian rivers. In river habitats, winter temperature limitations may exert a major control over the extent of microbial respiration (e.g., Yvon-Durocher et al., 2012) and DOM biodegradation. The higher %BDOC in winter than spring differs from observations in some other studies (Hosen et al., 2014), and likely represents the accumulation of biolabile DOM in the river that was subsequently accessed by microbes in the incubations conducted at room temperature. This difference could be due to the persistence of more bioavailable DOM in the river in winter under colder, dark conditions when there is extensive ice cover on the river and the microbial community is less metabolically active (Logozzo et al., 2021; Shousha et al., 2022), resulting in temperature-limitation that reduces winter DOC mineralization rates (Maavara et al., 2023). Removing temperature restrictions by incubating in the laboratory likely enabled the microbial community to access this bioavailable DOM pool more rapidly. These insights cannot be determined by simply measuring DOC concentrations that are typically collected as part of routine monitoring in Canadian Rivers (e.g., Johnston, Gunawardana, et al., 2022), so our exploration provides support for ongoing monitoring efforts, and a window into seldom-explored winter riverine processes and DOM cycling.

4.3. Most Fresh Leachate DOM Does Not Persist in the River Mainstem

The terrestrial to aquatic transitional zone of the Oldman River valley mainstem sampled here contains ample, highly bioavailable DOM sources on land and in the river itself (Figure 4). Yet, the mainstem of the river likely had a weak connection to these DOM sources during our study, or these DOM sources were remineralized or transformed in upstream impoundments, as indicated by the much lower bioavailability, lower DOC content, and distinct chemical composition of the riverine DOM at the sampling point (Figure 7). All leachate samples showed higher bioavailability compared to river samples (Figure 4). The turnover time and half-life of the DOC pool decreased with total leachable DOC (Figure 6), and the relative content of protein-like DOM, as the percent contribution of T and B peaks to F_{max} (Figure 5) for all leachate and river samples. These correlations are unsurprising, as protein-like DOM rich in N such as phenylpropyl (amino acid with lower aromaticity relative to A, M, and C peaks (Harfmann et al., 2019)) and other nutrients enhance microbial access to limiting nutrients and

heterotrophic DOC consumption rates (Mann et al., 2014; Shi et al., 2016), such that changes in DOM composition related to aromaticity and protein-like DOM content can decrease or increase, respectively, DOM bioavailability and turn-over rate ((Begum et al., 2023; A. A. Coble et al., 2016; F. Liu & Wang, 2022; Wickland et al., 2012). Yet composition and bioavailability of DOM sources were not the only factor controlling microbial metabolism in our incubations, as the concentration of DOM initially leached was the strongest correlate of DOC mineralization patterns (Figures 6 and 7). Since the total amount of leachable DOC was also strongly positively related to compositional shift toward protein-rich, less aromatic DOM, we cannot tease apart the influence of DOM quantity versus composition on BDOC patterns (Figure 7). It is possible that in other years with more precipitation in the watershed, more of the DOC-rich, bioavailable DOM sources in the river valley might be engaged, reservoir residence time and thus DOC uptake would decrease, and DOM cycling could differ from patterns observed here. Given that peak discharge in 2021 in the Oldman River was relatively low (~350 $m^3\ s^{-1}$) compared to some wetter years where peak discharge can exceed 1,000 or even ~4,000 $m^3\ s^{-1}$ (Johnston, Gunawardana, et al., 2022), we would expect years with higher flow through the mainstem location to potentially cause the DOM composition and bioavailability to shift toward other end members, possibly reflecting riparian vegetation signatures, or transport of headwater-derived DOM further downstream (e.g., Seidel et al., 2016). Therefore, we highlight that our observation in 2021 may be most representative of low flow, drought years where the river mainstem has limited engagement with riparian habitat along with increased residence time removing bioavailable DOM in upstream habitats.

Few (if any) studies have simultaneously documented the diversity of endmember DOM properties throughout the river valley; thus, we are uniquely able to show that autochthonous sources of DOM occupied an intermediate position in terms of bioavailability between fresh (vegetation) and stored (soil) DOM leachates. Leachate from fresh cottonwood leaves, shrubs, and grass showed the highest DOC bioavailability (83.8%–86.8%, Figure 4b) with a half-life of 9–12 days. This is similar to findings in other studies (Fellman et al., 2013; Hansen et al., 2016; Johnston et al., 2019), given that these sources supplied the greatest amount of DOC (Figure 6), and that protein-like DOM peaks B and T contributed 70.0%–81.8% to the % F_{max} of these leachates (Figure 3c), having very low aromaticity ($SUVA_{254}$ < 1.0 L mg C^{-1} m^{-1}, Table 2). The A:T ratio of terrestrial vegetation leachates (0.16–0.26), was in the range of values previously reported for vegetation (0.1–0.3, Hansen et al., 2016). Similar to our river valley samples, (Shelton et al., 2022) showed high BDOC of leachates from 8 distinct fresh tidal marsh plant species (average of 72.6%, range of 20.1%–86.1%). Next to fresh vegetation, the leachate from autochthonous DOM showed intermediate, but variable bioavailability that was highest for biofilm (80%), then macrophytes (67.4%), and FE products (50%). The lower bioavailability of FE DOM was surprising. Its high fraction of protein-like DOM (80.1%), low aromaticity ($SUVA_{254}$ = 0.60 L mg C^{-1} m^{-1}) and low A:T ratio (0.18) was similar to fresh terrestrial and aquatic vegetation and suggested that the DOM should be highly bioavailable. The amount of leachable DOC supplied was likely a dominant factor causing terrestrial plant leachates to sustain a greater amount and proportion of microbial DOC removal than river sources. Ultimately, although fish excrement has previously been stressed as important in the transformation of C and in supporting food webs (e.g., Q. Liu et al., 2022), to our knowledge, no study has framed this bioavailability relative to other river valley end member DOM sources to show that fish materials are actually intermediate in bioavailability relative to DOM from plant and biofilm communities.

While the least bioavailable group of leachates compared to vegetation and autochthonous sources, soil leachates from the Oldman River valley were highly bioavailable when compared to similar studies globally. The %BDOC from soil leachates were 23.9%–56.7% (mean = 44.8 ± 1.5%; Figure 4, Table 2), which was higher than globally averaged soil leachate bioavailability of 28.7% (F. Liu et al., 2021), but similar to that of wetland soils (23%–42%, Fellman et al., 2008). Our soil leachates had a range of 1.2–2.2 for A:T peak ratio values, which was extremely low compared to those from Hansen et al. (2016), who report soil leachates with high A:T ratios of 6.6. The $SUVA_{254}$ values for our soil leachates were on the low end of values from soils reported by Kelso et al. (2020), and lower than those for peatland soil leachates (3 L mg C^{-1} m^{-1}, Hansen et al., 2016) and forest soil leachates (2.2–3.9 L mg C^{-1} m^{-1}, Thieme et al., 2019). In these mineral-rich soils, the low aromaticity of leachates may be partly due to the precipitation and retention of more humic-like materials in soil particulate matter (Fellman et al., 2008; Shen et al., 2014; Ussiri & Johnson, 2003). Consequently, the reduced humic-like DOM content in our soil leachates is expected to sustain higher %BDOC (Fellman et al., 2008). These leachates are relatively rich in protein-like materials as indicated by low A:T peak ratios (discussed above) and the fact that both B and T peaks contributed roughly a quarter of the F_{max} values (Figure 3c). Finally, the elevated bioavailable protein-like

DOM content may be linked to lower soil microbial processing rates of dead plant materials in this arid region, especially during the extremely low precipitation conditions in the current drought period.

5. Conclusions

By documenting the seasonality in DOM content, composition, and bioavailability in the Oldman River and adjacent terrestrial habitats, we have provided new biogeochemical insights into the functioning of this economically and ecologically important watershed. Although the spring baseflow and freshet periods showed clear differences in lateral DOC export and the river valley contains multiple sources of highly bioavailable OM (soils, vegetation, and aquatic sources), riverine DOC concentration and DOM composition were largely decoupled from these sources and unresponsive to seasonal hydrology. As seen elsewhere, upstream reservoir creation likely modifies cycling of DOM in the river mainstem by enhancing DOM processing, reducing seasonal changes in DOM composition, and shifting the balance between auto- and allochthonous DOM cycling in the mainstem of the river. These insights have implications for understanding socially relevant processes including DOM impacts on the binding and transport of contaminants, drinking water purification, and the habitat features for important aquatic organisms (Asmala et al., 2013; Clark et al., 2008; Leenheer & Croué, 2003; Vanni, 2002). Given the limited existing information on riverine DOM cycling in western Canadian aquatic networks, our observations may reflect the typical patterns of DOM cycling in similar rivers transitioning from mountains to heavily impacted prairie ecoregions.

Data Availability Statement

All hydrometric data are publicly available from the Government of Canada National Water Data Archive (Station ID: 05AD007, https://wateroffice.ec.gc.ca/search/historical_e.html). Water chemistry data are available on the Federated Research Data Repository (Bogard & Zhou, 2024).

Acknowledgments
We thank Dr. Greg Pyle for the use of his GFAAS and Emma Neigel for taxonomic identification of terrestrial plant species. This project was supported by funding to M.J.B. from the University of Lethbridge, the Natural Sciences and Engineering Research Council of Canada – Discovery Grants program, the Canada Research Chairs program, the Canada Foundation for Innovation in partnership with the Government of Alberta, and the Alberta Innovates – Water Innovation Program. SEJ was supported by the National Science Foundation under Award 2053048.

References

Aitkenhead, J. A., & McDowell, W. H. (2000). Soil C:N ratio as a predictor of annual riverine DOC flux at local and global scales. *Global Biogeochemical Cycles*, *14*(1), 127–138. https://doi.org/10.1029/1999GB900083

Alberta Environment. (2007). Current and future water use in Alberta-Oldman River Basin (pp. 59–108).

Ankley, G. T., & Villeneuve, D. L. (2006). The fathead minnow in aquatic toxicology: Past, present and future. *Aquatic Toxicology*, *78*(1), 91–102. https://doi.org/10.1016/j.aquatox.2006.01.018

Asmala, E., Autio, R., Kaartokallio, H., Pitkänen, L., Stedmon, C. A., & Thomas, D. N. (2013). Bioavailability of riverine dissolved organic matter in three Baltic Sea estuaries and the effect of catchment land use. *Biogeosciences*, *10*(11), 6969–6986. https://doi.org/10.5194/bg-10-6969-2013

Barnes, R. T., Butman, D. E., Wilson, H. F., & Raymond, P. A. (2018). Riverine export of aged carbon driven by flow path depth and residence time. *Environmental Science & Technology*, *52*(3), 1028–1035. https://doi.org/10.1021/acs.est.7b04717

Battin, T. J., Besemer, K., Bengtsson, M. M., Romani, A. M., & Packmann, A. I. (2016). The ecology and biogeochemistry of stream biofilms. *Nature Reviews Microbiology*, *14*(4), 251–263. https://doi.org/10.1038/nrmicro.2016.15

Begum, M. S., Park, J.-H., Yang, L., Shin, K. H., & Hur, J. (2023). Optical and molecular indices of dissolved organic matter for estimating biodegradability and resulting carbon dioxide production in inland waters: A review. *Water Research*, *228*, 119362. https://doi.org/10.1016/j.watres.2022.119362

Bogard, M. J., & Zhou, X. (2024). Zhou et al. "Composition and bioreactivity of dissolved organic matter leachates from end members in a mountain to prairie transitional river valley" (version 1) [Dataset]. *Federated Research Data Repository*. https://doi.org/10.20383/103.0942

Butman, D., Raymond, P. A., Butler, K., & Aiken, G. (2012). Relationships between $\Delta^{14}C$ and the molecular quality of dissolved organic carbon in rivers draining to the coast from the conterminous United States. *Global Biogeochemical Cycles*, *26*(4), GB4014. https://doi.org/10.1029/2012gb004361

Butman, D., Stackpoole, S., Stets, E., McDonald, C. P., Clow, D. W., & Striegl, R. G. (2016). Aquatic carbon cycling in the conterminous United States and implications for terrestrial carbon accounting. *Proceedings of the National Academy of Sciences of the United States of America*, *113*(1), 58–63. https://doi.org/10.1073/pnas.1512651112

Byrne, J., Kienzle, S., Johnson, D., Duke, G., Gannon, V., Selinger, B., & Thomas, J. (2006). Current and future water issues in the Oldman River Basin of Alberta, Canada. *Water Science and Technology*, *53*(10), 327–334. https://doi.org/10.2166/wst.2006.328

Camino-Serrano, M., Gielen, B., Luyssaert, S., Ciais, P., Vicca, S., Guenet, B., et al. (2014). Linking variability in soil solution dissolved organic carbon to climate, soil type, and vegetation type. *Global Biogeochemical Cycles*, *28*(5), 497–509. https://doi.org/10.1002/2013gb004726

Carlson, C. A., & Hansell, D. A. (2015). Chapter 3 - DOM sources, sinks, reactivity, and budgets. In D. A. Hansell & C. A. Carlson (Eds.), *Biogeochemistry of marine dissolved organic matter* (2nd ed., pp. 65–126). Academic Press. https://doi.org/10.1016/B978-0-12-405940-5.00003-0

Catalán, N., Marcé, R., Kothawala, D. N., & Tranvik, L. J. (2016). Organic carbon decomposition rates controlled by water retention time across inland waters. *Nature Geoscience*, *9*(7), 501–504. https://doi.org/10.1038/ngeo2720

Chauvet, E. (1997). Leaf litter decomposition in large rivers: The case of the river garonne. *Limnética*, *13*(2), 65–70. https://doi.org/10.23818/limn.13.17

Clark, C. D., Litz, L. P., & Grant, S. B. (2008). Saltmarshes as a source of chromophoric dissolved organic matter (CDOM) to Southern California coastal waters. *Limnology and Oceanography*, *53*(5), 1923–1933. https://doi.org/10.4319/lo.2008.53.5.1923

Coble, A. A., Marcarelli, A. M., Kane, E. S., Toczydlowski, D., & Stottlemyer, R. (2016). Temporal patterns of dissolved organic matter biodegradability are similar across three rivers of varying size. *Journal of Geophysical Research: Biogeosciences*, *121*(6), 1617–1631. https://doi.org/10.1002/2015JG003218

Coble, P. G. (2007). Marine optical biogeochemistry: The chemistry of ocean color. *Chemical Reviews*, *107*(2), 402–418. https://doi.org/10.1021/cr050350+

Costerton, J. W. (1999). Introduction to biofilm. *International Journal of Antimicrobial Agents*, *11*(3–4), 217–221. https://doi.org/10.1016/S0924-8579(99)00018-7

Cross, P. M., & Anderson, A. M. (1989). An overview of water quality in the Oldman River basin (1984-1985) (p. 106). Environment (1971-1992, 1999-2011).

Culp, J. M., & Davies, R. W. (1982). Analysis of longitudinal zonation and the river continuum concept in the Oldman–South Saskatchewan River system. *Canadian Journal of Fisheries and Aquatic Sciences*, *39*(9), 1258–1266. https://doi.org/10.1139/f82-167

del Giorgio, P. A., & Davis, J. (2003). 17 - Patterns in dissolved organic matter lability and consumption across aquatic ecosystems. In S. E. G. Findlay & R. L. Sinsabaugh (Eds.), *Aquatic ecosystems* (pp. 399–424). Academic Press. https://doi.org/10.1016/B978-012256371-3/50018-4

del Giorgio, P. A., & Pace, M. L. (2008). Relative independence of organic carbon transport and processing in a large temperate river: The Hudson River as both pipe and reactor. *Limnology and Oceanography*, *53*(1), 185–197. https://doi.org/10.4319/lo.2008.53.1.0185

Dittmar, T., & Stubbins, A. (2014). Dissolved organic matter in aquatic systems. In *Treatise on geochemistry* (pp. 125–156). https://doi.org/10.1016/b978-0-08-095975-7.01010-x

Dobbs, R. A., Wise, R. H., & Dean, R. B. (1972). The use of ultra-violet absorbance for monitoring the total organic carbon content of water and wastewater. *Water Research*, *6*(10), 1173–1180. https://doi.org/10.1016/0043-1354(72)90017-6

Du, Y., Chen, F., Xiao, K., Song, C., He, H., Zhang, Q., et al. (2021). Water residence time and temperature drive the dynamics of dissolved organic matter in Alpine Lakes in the Tibetan Plateau. *Global Biogeochemical Cycles*, *35*(11), e2020GB006908. https://doi.org/10.1029/2020GB006908

Duffy, W. G. (1998). Population dynamics, production, and prey consumption of fathead minnows (*Pimephales promelas*) in prairie wetlands: A bioenergetics approach. *Canadian Journal of Fisheries and Aquatic Sciences*, *55*(1), 15–27. https://doi.org/10.1139/f97-204

Farag, A. M., Nimick, D. A., Kimball, B. A., Church, S. E., Harper, D. D., & Brumbaugh, W. G. (2007). Concentrations of metals in water, sediment, biofilm, benthic macroinvertebrates, and fish in the Boulder River watershed, Montana, and the role of colloids in metal uptake. *Archives of Environmental Contamination and Toxicology*, *52*(3), 397–409. https://doi.org/10.1007/s00244-005-0021-z

Fellman, J. B., D'Amore, D. V., Hood, E., & Boone, R. D. (2008). Fluorescence characteristics and biodegradability of dissolved organic matter in forest and wetland soils from coastal temperate watersheds in southeast Alaska. *Biogeochemistry*, *88*(2), 169–184. https://doi.org/10.1007/s10533-008-9203-x

Fellman, J. B., Hood, E., & Robert, G. M. S. (2010). Fluorescence spectroscopy opens new windows into dissolved organic matter dynamics in freshwater ecosystems: A review. *Limnology and Oceanography*, *55*(6), 2452–2462. https://doi.org/10.4319/lo.2010.55.6.2452

Fellman, J. B., Petrone, K. C., & Grierson, P. F. (2013). Leaf litter age, chemical quality, and photodegradation control the fate of leachate dissolved organic matter in a dryland river. *Journal of Arid Environments*, *89*, 30–37. https://doi.org/10.1016/j.jaridenv.2012.10.011

Fellman, J. B., Spencer, R. G. M., Raymond, P. A., Pettit, N. E., Skrzypek, G., Hernes, P. J., & Grierson, P. F. (2014). Dissolved organic carbon biolability decreases along with its modernization in fluvial networks in an ancient landscape. *Ecology*, *95*(9), 2622–2632. https://doi.org/10.1890/13-1360.1

Findlay, S., & Sinsabaugh, R. L. (2003). *Aquatic ecosystems: Interactivity of dissolved organic matter* (Vol. xx, p. 512). Academic Press.

Flanagan, L. B., Orchard, T. E., Logie, G. S. J., Coburn, C. A., & Rood, S. B. (2017). Water use in a riparian cottonwood ecosystem: Eddy covariance measurements and scaling along a river corridor. *Agricultural and Forest Meteorology*, *232*, 332–348. https://doi.org/10.1016/j.agrformet.2016.08.024

Flemming, H.-C. (1995). Sorption sites in biofilms. *Water Science and Technology*, *32*(8), 27–33. https://doi.org/10.1016/0273-1223(96)00004-2

Grill, G., Lehner, B., Thieme, M., Geenen, B., Tickner, D., Antonelli, F., et al. (2019). Mapping the world's free-flowing rivers. *Nature*, *569*(7755), 215–221. https://doi.org/10.1038/s41586-019-1111-9

Guillemette, F., & del Giorgio, P. A. (2011). Reconstructing the various facets of dissolved organic carbon bioavailability in freshwater ecosystems. *Limnology and Oceanography*, *56*(2), 734–748. https://doi.org/10.4319/lo.2011.56.2.0734

Hanley, K. W., Wollheim, W. M., Salisbury, J., Huntington, T., & Aiken, G. (2013). Controls on dissolved organic carbon quantity and chemical character in temperate rivers of North America. *Global Biogeochemical Cycles*, *27*(2), 492–504. https://doi.org/10.1002/gbc.20044

Hansen, A. M., Kraus, T. E. C., Pellerin, B. A., Fleck, J. A., Downing, B. D., & Bergamaschi, B. A. (2016). Optical properties of dissolved organic matter (DOM): Effects of biological and photolytic degradation. *Limnology and Oceanography*, *61*(3), 1015–1032. https://doi.org/10.1002/lno.10270

Harfmann, J. L., Guillemette, F., Kaiser, K., Spencer, R. G. M., Chuang, C.-Y., & Hernes, P. J. (2019). Convergence of terrestrial dissolved organic matter composition and the role of microbial buffering in aquatic ecosystems. *Journal of Geophysical Research: Biogeosciences*, *124*(10), 3125–3142. https://doi.org/10.1029/2018JG004997

Helms, J. R., Stubbins, A., Ritchie, J. D., Minor, E. C., Kieber, D. J., & Mopper, K. (2008). Absorption spectral slopes and slope ratios as indicators of molecular weight, source, and photobleaching of chromophoric dissolved organic matter. *Limnology and Oceanography*, *53*(3), 955–969. https://doi.org/10.4319/lo.2008.53.3.0955

Hosen, J. D., Aho, K. S., Appling, A. P., Creech, E. C., Fair, J. H., Hall, R. O., et al. (2019). Enhancement of primary production during drought in a temperate watershed is greater in larger rivers than headwater streams. *Limnology and Oceanography*, *64*(4), 1458–1472. https://doi.org/10.1002/lno.11127

Hosen, J. D., Aho, K. S., Fair, J. H., Kyzivat, E. D., Matt, S., Morrison, J., et al. (2020). Source switching maintains dissolved organic matter chemostasis across discharge levels in a large temperate River Network. *Ecosystems*, *24*(2), 227–247. https://doi.org/10.1007/s10021-020-00514-7

Hosen, J. D., Allen, G. H., Amatulli, G., Breitmeyer, S., Cohen, M. J., Crump, B. C., et al. (2021). River network travel time is correlated with dissolved organic matter composition in rivers of the contiguous United States. *Hydrological Processes*, *35*(5), e14124. https://doi.org/10.1002/hyp.14124

Hosen, J. D., McDonough, O. T., Febria, C. M., & Palmer, M. A. (2014). Dissolved organic matter quality and bioavailability changes across an urbanization gradient in headwater streams. *Environmental Science & Technology*, *48*(14), 7817–7824. https://doi.org/10.1021/es501422z

Hullar, M. A. J., Kaplan, L. A., & Stahl, D. A. (2006). Recurring seasonal dynamics of microbial communities in stream habitats. *Applied and Environmental Microbiology*, *72*(1), 713–722. https://doi.org/10.1128/AEM.72.1.713-722.2006

Hutchins, R. H. S., Aukes, P., Schiff, S. L., Dittmar, T., Prairie, Y. T., & del Giorgio, P. A. (2017). The optical, chemical, and molecular dissolved organic matter succession along a boreal soil-stream-river continuum. *Journal of Geophysical Research: Biogeosciences*, *122*(11), 2892–2908. https://doi.org/10.1002/2017jg004094

Johnston, S. E., Bogard, M. J., Rogers, J. A., Butman, D., Striegl, R. G., Dornblaser, M., & Spencer, R. G. M. (2019). Constraining dissolved organic matter sources and temporal variability in a model sub-Arctic lake. *Biogeochemistry*, *146*(3), 271–292. https://doi.org/10.1007/s10533-019-00619-9

Johnston, S. E., Finlay, K., Spencer, R. G. M., Butman, D. E., Metz, M., Striegl, R., & Bogard, M. J. (2022). Zooplankton release complex dissolved organic matter to aquatic environments. *Biogeochemistry*, *157*(3), 313–325. https://doi.org/10.1007/s10533-021-00876-7

Johnston, S. E., Gunawardana, P. V. S. L., Rood, S. B., & Bogard, M. J. (2022). Multidecadal trends in organic carbon flux through a grassland river network shaped by human controls and climatic cycles. *Geophysical Research Letters*, *49*(4), e2021GL096885. https://doi.org/10.1029/2021GL096885

Johnston, S. E., Shorina, N., Bulygina, E., Vorobjeva, T., Chupakova, A., Klimov, S. I., et al. (2018). Flux and seasonality of dissolved organic matter from the Northern Dvina (Severnaya Dvina) river, Russia. *Journal of Geophysical Research: Biogeosciences*, *123*(3), 1041–1056. https://doi.org/10.1002/2017jg004337

Jokinen, C. C., Edge, T. A., Koning, W., Laing, C. R., Lapen, D. R., Miller, J., et al. (2012). Spatial and temporal drivers of zoonotic pathogen contamination of an agricultural watershed. *Journal of Environmental Quality*, *41*(1), 242–252. https://doi.org/10.2134/jeq2011.0203

Kaiser, K., & Kalbitz, K. (2012). Cycling downwards – Dissolved organic matter in soils. *Soil Biology and Biochemistry*, *52*, 29–32. https://doi.org/10.1016/j.soilbio.2012.04.002

Kamjunke, N., Herzsprung, P., & Neu, T. R. (2015). Quality of dissolved organic matter affects planktonic but not biofilm bacterial production in streams. *Science of the Total Environment*, *506–507*, 353–360. https://doi.org/10.1016/j.scitotenv.2014.11.043

Kao, L. S., & Green, C. E. (2008). Analysis of variance: Is there a difference in means and what does it mean? *Journal of Surgical Research*, *144*(1), 158–170. https://doi.org/10.1016/j.jss.2007.02.053

Kelso, J. E., Rosi, E. J., & Baker, M. A. (2020). Towards more realistic estimates of DOM decay in streams: Incubation methods, light, and non-additive effects. *Freshwater Science*, *39*(3), 559–575. https://doi.org/10.1086/710218

Kindler, R., Siemens, J., Kaiser, K., Walmsley, D. C., Bernhofer, C., Buchmann, N., et al. (2011). Dissolved carbon leaching from soil is a crucial component of the net ecosystem carbon balance. *Global Change Biology*, *17*(2), 1167–1185. https://doi.org/10.1111/j.1365-2486.2010.02282.x

Koning, C. W., Saffran, K. A., Little, J. L., & Fent, L. (2006). Water quality monitoring: The basis for watershed management in the Oldman River Basin, Canada. *Water Science and Technology*, *53*(10), 153–161. https://doi.org/10.2166/wst.2006.308

LaBrie, R., Lapierre, J. F., & Maranger, R. (2020). Contrasting patterns of labile and semilabile dissolved organic carbon from continental waters to the open ocean. *Journal of Geophysical Research: Biogeosciences*, *125*(2), e2019JG005300. https://doi.org/10.1029/2019JG005300

Lapierre, J. F., & del Giorgio, P. A. (2014). Partial coupling and differential regulation of biologically and photochemically labile dissolved organic carbon across boreal aquatic networks. *Biogeosciences*, *11*(20), 5969–5985. https://doi.org/10.5194/bg-11-5969-2014

Lapierre, J.-F., & Frenette, J.-J. (2009). Effects of macrophytes and terrestrial inputs on fluorescent organic matter in a large river system. *Aquatic Sciences*, *71*(1), 15–24. https://doi.org/10.1007/s00027-009-9133-2

Leenheer, J., & Croué, J. (2003). Characterizing aquatic dissolved organic matter: Understanding the unknown structures is key to better treatment of drinking water. *Environmental Science & Technology*, *37*(1), 18A–26A. https://doi.org/10.1021/es032333c

Li, P., & Hur, J. (2017). Utilization of UV-vis spectroscopy and related data analyses for dissolved organic matter (DOM) studies: A review. *Critical Reviews in Environmental Science and Technology*, *47*(3), 131–154. https://doi.org/10.1080/10643389.2017.1309186

Lidman, J., Jonsson, M., Burrows, R. M., Bundschuh, M., & Sponseller, R. A. (2017). Composition of riparian litter input regulates organic matter decomposition: Implications for headwater stream functioning in a managed forest landscape. *Ecology and Evolution*, *7*(4), 1068–1077. https://doi.org/10.1002/ece3.2726

Liu, F., & Wang, D. (2022). Dissolved organic carbon concentration and biodegradability across the global rivers: A meta-analysis. *Science of the Total Environment*, *818*, 151828. https://doi.org/10.1016/j.scitotenv.2021.151828

Liu, F., Wang, D., Zhang, B., & Huang, J. (2021). Concentration and biodegradability of dissolved organic carbon derived from soils: A global perspective. *Science of the Total Environment*, *754*, 142378. https://doi.org/10.1016/j.scitotenv.2020.142378

Liu, Q., Zhou, L., Wu, Y., Huang, H., He, X., Gao, N., & Zhang, L. (2022). Quantification of the carbon released by a marine fish using a carbon release model and radiocarbon. *Marine Pollution Bulletin*, *181*, 113908. https://doi.org/10.1016/j.marpolbul.2022.113908

Logozzo, L., Tzortziou, M., Neale, P., & Clark, J. B. (2021). Photochemical and microbial degradation of chromophoric dissolved organic matter exported from tidal marshes. *Journal of Geophysical Research: Biogeosciences*, *126*(4), e2020JG005744. https://doi.org/10.1029/2020JG005744

Logozzo, L. A., Hosen, J. D., McArthur, J., & Raymond, P. A. (2023). Distinct drivers of two size fractions of operationally dissolved iron in a temperate river. *Limnology and Oceanography*, *68*(6), 1185–1200. https://doi.org/10.1002/lno.12338

Logozzo, L. A., Martin, J. W., McArthur, J., & Raymond, P. A. (2022). Contributions of Fe(III) to UV–vis absorbance in river water: A case study on the Connecticut River and argument for the systematic tandem measurement of Fe(III) and CDOM. *Biogeochemistry*, *160*(1), 17–33. https://doi.org/10.1007/s10533-022-00937-5

Maas, A. E., Liu, S., Bolaños, L. M., Widner, B., Parsons, R., Kujawinski, E. B., et al. (2020). Migratory zooplankton excreta and its influence on prokaryotic communities. *Frontiers in Marine Science*, *7*(573268), 1–15. https://doi.org/10.3389/fmars.2020.573268

Maavara, T., Brinkerhoff, C., Hosen, J., Aho, K., Logozzo, L., Saiers, J., et al. (2023). Watershed DOC uptake occurs mostly in lakes in the summer and in rivers in the winter. *Limnology and Oceanography*, *68*(3), 735–751. https://doi.org/10.1002/lno.12306

Maavara, T., Chen, Q., Van Meter, K., Brown, L. E., Zhang, J., Ni, J., & Zarfl, C. (2020). River dam impacts on biogeochemical cycling. *Nature Reviews Earth & Environment*, *1*(2), 103–116. https://doi.org/10.1038/s43017-019-0019-0

Mangal, V., Stock, N. L., & Guéguen, C. (2016). Molecular characterization of phytoplankton dissolved organic matter (DOM) and sulfur components using high resolution Orbitrap mass spectrometry. *Analytical and Bioanalytical Chemistry*, *408*(7), 1891–1900. https://doi.org/10.1007/s00216-015-9295-9

Mann, P. J., Sobczak, W. V., LaRue, M. M., Bulygina, E., Davydova, A., Vonk, J. E., et al. (2014). Evidence for key enzymatic controls on metabolism of Arctic river organic matter. *Global Change Biology*, *20*(4), 1089–1100. https://doi.org/10.1111/gcb.12416

Massicotte, P., Asmala, E., Stedmon, C., & Markager, S. (2017). Global distribution of dissolved organic matter along the aquatic continuum: Across rivers, lakes and oceans. *Science of the Total Environment*, *609*, 180–191. https://doi.org/10.1016/j.scitotenv.2017.07.076

McKnight, D. M., Boyer, E. W., Westerhoff, P. K., Doran, P. T., Kulbe, T., & Andersen, D. T. (2001). Spectrofluorometric characterization of dissolved organic matter for indication of precursor organic material and aromaticity. *Limnology and Oceanography*, *46*(1), 38–48. https://doi.org/10.4319/lo.2001.46.1.0038

Miller, M. P. (2012). The influence of reservoirs, climate, land use and hydrologic conditions on loads and chemical quality of dissolved organic carbon in the Colorado River. *Water Resources Research*, *48*(12), W00M02. https://doi.org/10.1029/2012WR012312
Minor, E. C., Swenson, M. M., Mattson, B. M., & Oyler, A. R. (2014). Structural characterization of dissolved organic matter: A review of current techniques for isolation and analysis. *Environmental Science: Processes & Impacts*, *16*(9), 2064–2079. https://doi.org/10.1039/c4em00062e
Moran, M. A., & Covert, J. S. (2003). 10 - Photochemically mediated linkages between dissolved organic matter and bacterioplankton. In S. E. G. Findlay & R. L. Sinsabaugh (Eds.), *Aquatic ecosystems* (pp. 243–262). Academic Press. https://doi.org/10.1016/B978-012256371-3/50011-1
Moran, M. A., Sheldon, W. M., & Sheldon, J. E. (1999). Biodegradation of riverine dissolved organic carbon in five estuaries of the southeastern United States. *Estuaries*, *22*(1), 55–64. https://doi.org/10.2307/1352927
Murphy, K. R., Butler, K. D., Spencer, R. G. M., Stedmon, C. A., Boehme, J. R., & Aiken, G. R. (2010). Measurement of dissolved organic matter fluorescence in aquatic environments: An interlaboratory comparison. *Environmental Science & Technology*, *44*(24), 9405–9412. https://doi.org/10.1021/es102362t
Murphy, K. R., Stedmon, C. A., Graeber, D., & Bro, R. (2013). Fluorescence spectroscopy and multi-way techniques. PARAFAC. *Analytical Methods*, *5*(23), 6557. https://doi.org/10.1039/c3ay41160e
Namieśnik, J., & Rabajczyk, A. (2015). The speciation and physico-chemical forms of metals in surface waters and sediments. *Chemical Speciation and Bioavailability*, *22*(1), 1–24. https://doi.org/10.3184/095422910x12632119406391
O'Donnell, J. A., Aiken, G. R., Swanson, D. K., Panda, S., Butler, K. D., & Baltensperger, A. P. (2016). Dissolved organic matter composition of Arctic rivers: Linking permafrost and parent material to riverine carbon. *Global Biogeochemical Cycles*, *30*(12), 1811–1826. https://doi.org/10.1002/2016GB005482
Ohno, T. (2002). Fluorescence inner-filtering correction for determining the humification index of dissolved organic matter. *Environmental Science & Technology*, *36*(4), 742–746. https://doi.org/10.1021/es0155276
Oliver, A. A., Spencer, R. G. M., Deas, M. L., & Dahlgren, R. A. (2016). Impact of seasonality and anthropogenic impoundments on dissolved organic matter dynamics in the Klamath River (Oregon/California, USA). *Journal of Geophysical Research: Biogeosciences*, *121*(7), 1946–1958. https://doi.org/10.1002/2016jg003497
Parr, T. B., Capps, K. A., Inamdar, S. P., Metcalf, K. A., & Leroux, S. (2018). Animal-mediated organic matter transformation: Aquatic insects as a source of microbially bioavailable organic nutrients and energy. *Functional Ecology*, *33*(3), 524–535. https://doi.org/10.1111/1365-2435.13242
Pinsonneault, A. J., Moore, T. R., Roulet, N. T., & Lapierre, J.-F. (2016). Biodegradability of vegetation-derived dissolved organic carbon in a cool temperate ombrotrophic bog. *Ecosystems*, *19*(6), 1023–1036. https://doi.org/10.1007/s10021-016-9984-z
Poulin, B. A., Ryan, J. N., & Aiken, G. R. (2014). Effects of iron on optical properties of dissolved organic matter. *Environmental Science & Technology*, *48*(17), 10098–10106. https://doi.org/10.1021/es502670r
Pucher, M., Wünsch, U., Weigelhofer, G., Murphy, K., Hein, T., & Graeber, D. (2019). staRdom: Versatile software for analyzing spectroscopic data of dissolved organic matter in R. *Water*, *11*(11), 2366. https://doi.org/10.3390/w11112366
Raymond, P. A., Saiers, J. E., & Sobczak, W. V. (2016). Hydrological and biogeochemical controls on watershed dissolved organic matter transport: Pulse-shunt concept. *Ecology*, *97*(1), 5–16. https://doi.org/10.1890/14-1684.1
RCoreTeam. (2021). *R: A language and environment for statistical computing*. Foundation for Statistical Computing.
Risse-Buhl, U., Trefzger, N., Seifert, A. G., Schönborn, W., Gleixner, G., & Küsel, K. (2012). Tracking the autochthonous carbon transfer in stream biofilm food webs. *FEMS Microbiology Ecology*, *79*(1), 118–131. https://doi.org/10.1111/j.1574-6941.2011.01202.x
Rock, L., & Mayer, B. (2006). Nitrogen budget for the Oldman River Basin, Southern Alberta, Canada. *Nutrient Cycling in Agroecosystems*, *75*(1–3), 147–162. https://doi.org/10.1007/s10705-006-9018-x
Rock, L., & Mayer, B. (2007). Isotope hydrology of the Oldman River Basin, Southern Alberta, Canada. *Hydrological Processes*, *21*(24), 3301–3315. https://doi.org/10.1002/hyp.6545
Romaní, A. M., Guasch, H., Munoz, I., Ruana, J., Vilalta, E., Schwartz, T., et al. (2004). Biofilm structure and function and possible implications for riverine DOC dynamics. *Microbial Ecology*, *47*(4), 316–328. https://doi.org/10.1007/s00248-003-2019-2
Sabater, S., Guasch, H., Ricart, M., Romani, A., Vidal, G., Klunder, C., & Schmitt-Jansen, M. (2007). Monitoring the effect of chemicals on biological communities. The biofilm as an interface. *Analytical and Bioanalytical Chemistry*, *387*(4), 1425–1434. https://doi.org/10.1007/s00216-006-1051-8
Schindler, D. (2019). Past, present and future challenges to management of freshwater quality in Canada. *Water Quality in the Americas*, *128*.
Schindler, D. W. (2001). The cumulative effects of climate warming and other human stresses on Canadian freshwaters in the new millennium. *Canadian Journal of Fisheries and Aquatic Sciences*, *58*(1), 18–29. https://doi.org/10.1139/f00-179
Schmitz, O. J., Raymond, P. A., Estes, J. A., Kurz, W. A., Holtgrieve, G. W., Ritchie, M. E., et al. (2014). Animating the carbon cycle. *Ecosystems*, *17*(2), 344–359. https://doi.org/10.1007/s10021-013-9715-7
Seidel, M., Dittmar, T., Ward, N. D., Krusche, A. V., Richey, J. E., Yager, P. L., & Medeiros, P. M. (2016). Seasonal and spatial variability of dissolved organic matter composition in the lower Amazon River. *Biogeochemistry*, *131*(3), 281–302. https://doi.org/10.1007/s10533-016-0279-4
Seifert, A. G., Roth, V. N., Dittmar, T., Gleixner, G., Breuer, L., Houska, T., & Marxsen, J. (2016). Comparing molecular composition of dissolved organic matter in soil and stream water: Influence of land use and chemical characteristics. *Science of the Total Environment*, *571*, 142–152. https://doi.org/10.1016/j.scitotenv.2016.07.033
Shelton, S., Neale, P., Pinsonneault, A., & Tzortziou, M. (2022). Biodegradation and photodegradation of vegetation-derived dissolved organic matter in tidal marsh ecosystems. *Estuaries and Coasts*, *45*(5), 1324–1342. https://doi.org/10.1007/s12237-021-00982-7
Shen, Y., Chapelle, F. H., Strom, E. W., & Benner, R. (2014). Origins and bioavailability of dissolved organic matter in groundwater. *Biogeochemistry*, *122*(1), 61–78. https://doi.org/10.1007/s10533-014-0029-4
Shi, J., Cui, H., Jia, L., Qiu, L., Zhao, Y., Wei, Z., et al. (2016). Bioavailability of riverine dissolved organic carbon and nitrogen in the Heilongjiang watershed of northeastern China. *Environmental Monitoring and Assessment*, *188*(2), 113. https://doi.org/10.1007/s10661-016-5120-y
Shousha, S., Maranger, R., & Lapierre, J.-F. (2022). Contrasting seasons and land uses alter riverine dissolved organic matter composition. *Biogeochemistry*, *161*(2), 207–226. https://doi.org/10.1007/s10533-022-00979-9
Shultz, M., Pellerin, B., Aiken, G., Martin, J., & Raymond, P. (2018). High frequency data exposes nonlinear seasonal controls on dissolved organic matter in a large watershed. *Environmental Science & Technology*, *52*(10), 5644–5652. https://doi.org/10.1021/acs.est.7b04579
Singh, S., Inamdar, S., Mitchell, M., & McHale, P. (2014). Seasonal pattern of dissolved organic matter (DOM) in watershed sources: Influence of hydrologic flow paths and autumn leaf fall. *Biogeochemistry*, *118*(1), 321–337. https://doi.org/10.1007/s10533-013-9934-1

Stanley, E. H., Powers, S. M., Lottig, N. R., Buffam, I., & Crawford, J. T. (2012). Contemporary changes in dissolved organic carbon (DOC) in human-dominated rivers: Is there a role for DOC management? *Freshwater Biology*, *57*(s1), 26–42. https://doi.org/10.1111/j.1365-2427.2011.02613.x

Tan, X., & Gan, T. Y. (2015). Contribution of human and climate change impacts to changes in streamflow of Canada. *Scientific Reports*, *5*(1), 17767. https://doi.org/10.1038/srep17767

Tank, S. E., Fellman, J. B., Hood, E., & Kritzberg, E. S. (2018). Beyond respiration: Controls on lateral carbon fluxes across the terrestrial-aquatic interface. *Limnology and Oceanography Letters*, *3*(3), 76–88. https://doi.org/10.1002/lol2.10065

Tanzeeba, S., & Gan, T. Y. (2012). Potential impact of climate change on the water availability of South Saskatchewan River Basin. *Climatic Change*, *112*(2), 355–386. https://doi.org/10.1007/s10584-011-0221-7

Thieme, L., Graeber, D., Hofmann, D., Bischoff, S., Schwarz, M. T., Steffen, B., et al. (2019). Dissolved organic matter characteristics of deciduous and coniferous forests with variable management: Different at the source, aligned in the soil. *Biogeosciences*, *16*(7), 1411–1432. https://doi.org/10.5194/bg-16-1411-2019

Thorp, J. H., Thoms, M. C., & Delong, M. D. (2006). The riverine ecosystem synthesis: Biocomplexity in river networks across space and time. *River Research and Applications*, *22*(2), 123–147. https://doi.org/10.1002/rra.901

Ulseth, A. J., & Hall, R. O. (2015). Dam tailwaters compound the effects of reservoirs on the longitudinal transport of organic carbon in an arid river. *Biogeosciences*, *12*(14), 4345–4359. https://doi.org/10.5194/bg-12-4345-2015

Ussiri, D. A. N., & Johnson, C. E. (2003). Characterization of organic matter in a northern hardwood forest soil by ^{13}C NMR spectroscopy and chemical methods. *Geoderma*, *111*(1), 123–149. https://doi.org/10.1016/S0016-7061(02)00257-4

van den Berg, L. J. L., Shotbolt, L., & Ashmore, M. R. (2012). Dissolved organic carbon (DOC) concentrations in UK soils and the influence of soil, vegetation type and seasonality. *Science of the Total Environment*, *427–428*, 269–276. https://doi.org/10.1016/j.scitotenv.2012.03.069

Vanni, M. J. (2002). Nutrient cycling by animals in freshwater ecosystems. *Annual Review of Ecology and Systematics*, *33*(1), 341–370. https://doi.org/10.1146/annurev.ecolsys.33.010802.150519

Vannote, R. L., Minshall, G. W., Cummins, K. W., Sedell, J. R., & Cushing, C. E. (1980). The river continuum concept. *Canadian Journal of Fisheries and Aquatic Sciences*, *37*(1), 130–137. https://doi.org/10.1139/f80-017

Vaughn, D. R., Kellerman, A. M., Wickland, K. P., Striegl, R. G., Podgorski, D. C., Hawkings, J. R., et al. (2021). Anthropogenic landcover impacts fluvial dissolved organic matter composition in the Upper Mississippi River Basin. *Biogeochemistry*, *164*(1), 117–141. https://doi.org/10.1007/s10533-021-00852-1

Vaughn, D. R., Kellerman, A. M., Wickland, K. P., Striegl, R. G., Podgorski, D. C., Hawkings, J. R., et al. (2023). Bioavailability of dissolved organic matter varies with anthropogenic landcover in the Upper Mississippi River Basin. *Water Research*, *229*, 119357. https://doi.org/10.1016/j.watres.2022.119357

Vorosmarty, C. J., McIntyre, P. B., Gessner, M. O., Dudgeon, D., Prusevich, A., Green, P., et al. (2010). Global threats to human water security and river biodiversity. *Nature*, *467*(7315), 555–561. https://doi.org/10.1038/nature09440

Wagner, S., Riedel, T., Niggemann, J., Vahatalo, A. V., Dittmar, T., & Jaffe, R. (2015). Linking the molecular signature of heteroatomic dissolved organic matter to watershed characteristics in world rivers. *Environmental Science & Technology*, *49*(23), 13798–13806. https://doi.org/10.1021/acs.est.5b00525

Wang, F., Maberly, S. C., Wang, B., & Liang, X. (2018). Effects of dams on riverine biogeochemical cycling and ecology. *Inland Waters*, *8*(2), 130–140. https://doi.org/10.1080/20442041.2018.1469335

Ward, N. D., Sawakuchi, H. O., Neu, V., Less, D. F. S., Valerio, A. M., Cunha, A. C., et al. (2018). Velocity-amplified microbial respiration rates in the lower Amazon River. *Limnology and Oceanography Letters*, *3*(3), 265–274. https://doi.org/10.1002/lol2.10062

Weishaar, J. L., Aiken, G. R., Bergamaschi, B. A., Fram, M. S., Fujii, R., & Mopper, K. (2003). Evaluation of specific ultraviolet absorbance as an indicator of the chemical composition and reactivity of dissolved organic carbon. *Environmental Science & Technology*, *37*(20), 4702–4708. https://doi.org/10.1021/es030360x

Wickens, G. E. (1998). Arid and semi-arid environments of the world. In G. E. Wickens (Ed.), *Ecophysiology of economic plants in arid and semi-arid lands* (pp. 5–15). Springer Berlin Heidelberg. https://doi.org/10.1007/978-3-662-03700-3_2

Wickland, K. P., Aiken, G. R., Butler, K., Dornblaser, M. M., Spencer, R. G. M., & Striegl, R. G. (2012). Biodegradability of dissolved organic carbon in the Yukon River and its tributaries: Seasonality and importance of inorganic nitrogen. *Global Biogeochemical Cycles*, *26*(4), GB0E03. https://doi.org/10.1029/2012GB004342

Wilson, H. F., & Xenopoulos, M. A. (2008). Effects of agricultural land use on the composition of fluvial dissolved organic matter. *Nature Geoscience*, *2*(1), 37–41. https://doi.org/10.1038/ngeo391

Xenopoulos, M. A., Barnes, R. T., Boodoo, K. S., Butman, D., Catalán, N., D'Amario, S. C., et al. (2021). How humans alter dissolved organic matter composition in freshwater: Relevance for the Earth's biogeochemistry. *Biogeochemistry*, *154*(2), 323–348. https://doi.org/10.1007/s10533-021-00753-3

Xenopoulos, M. A., Lodge, D. M., Frentress, J., Kreps, T. A., Bridgham, S. D., Grossman, E., & Jackson, C. J. (2003). Regional comparisons of watershed determinants of dissolved organic carbon in temperate lakes from the Upper Great Lakes region and selected regions globally. *Limnology and Oceanography*, *48*(6), 2321–2334. https://doi.org/10.4319/lo.2003.48.6.2321

Yvon-Durocher, G., Caffrey, J. M., Cescatti, A., Dossena, M., Giorgio, P. d., Gasol, J. M., et al. (2012). Reconciling the temperature dependence of respiration across timescales and ecosystem types. *Nature*, *487*(7408), 472–476. https://doi.org/10.1038/nature11205

Zhang, Y., Liu, X., Wang, M., & Qin, B. (2013). Compositional differences of chromophoric dissolved organic matter derived from phytoplankton and macrophytes. *Organic Geochemistry*, *55*, 26–37. https://doi.org/10.1016/j.orggeochem.2012.11.007

Zhou, X., Johnston, S. E., & Bogard, M. J. (2023). Organic matter cycling in a model restored wetland receiving complex effluent. *Biogeochemistry*, *162*(2), 237–255. https://doi.org/10.1007/s10533-022-01002-x